(12) INTERNATIONAL APPLICATION PUBLISHED UNDER THE PATENT COOPERATION TREATY (PCT)

(19) World Intellectual Property Organization
International Bureau

(43) International Publication Date
14 December 2017 (14.12.2017)

WIPO | PCT

(10) International Publication Number
WO 2017/214604 A1

(51) International Patent Classification:
A61B 5/00 (2006.01) *G01J 3/44* (2006.01)
G01J 3/00 (2006.01)

(21) International Application Number:
PCT/US2017/036915

(22) International Filing Date:
10 June 2017 (10.06.2017)

(25) Filing Language: English

(26) Publication Language: English

(30) Priority Data:
62/348,502 10 June 2016 (10.06.2016) US

(71) Applicant: **THE TRUSTEES OF COLUMBIA UNIVERSITY IN THE CITY OF NEW YORK** [US/US]; 412 Low Memorial Library, 535 West 116th Street, Mail Code 4308, New York, New York 10027 (US).

(72) Inventors: **VUKELIC, Sinisa**; 531 W 112th Street, Apartment 3D, New York, New York 10025 (US). **ATESHIAN, Gerard A.**; 440 Riverside Drive, Apt. 82, New York, New York 10027 (US).

(74) Agent: **CATAN, Mark A.**; Potomac Law Group, PLLC, 5335 Wisconsin Ave Suite 440, Washington, District of Columbia 20015 (US).

(81) Designated States *(unless otherwise indicated, for every kind of national protection available)*: AE, AG, AL, AM, AO, AT, AU, AZ, BA, BB, BG, BH, BN, BR, BW, BY, BZ, CA, CH, CL, CN, CO, CR, CU, CZ, DE, DJ, DK, DM, DO, DZ, EC, EE, EG, ES, FI, GB, GD, GE, GH, GM, GT, HN, HR, HU, ID, IL, IN, IR, IS, JO, JP, KE, KG, KH, KN, KP, KR, KW, KZ, LA, LC, LK, LR, LS, LU, LY, MA, MD, ME, MG, MK, MN, MW, MX, MY, MZ, NA, NG, NI, NO, NZ, OM, PA, PE, PG, PH, PL, PT, QA, RO, RS, RU, RW, SA, SC, SD, SE, SG, SK, SL, SM, ST, SV, SY, TH, TJ, TM, TN, TR, TT, TZ, UA, UG, US, UZ, VC, VN, ZA, ZM, ZW.

(84) Designated States *(unless otherwise indicated, for every kind of regional protection available)*: ARIPO (BW, GH, GM, KE, LR, LS, MW, MZ, NA, RW, SD, SL, ST, SZ, TZ, UG, ZM, ZW), Eurasian (AM, AZ, BY, KG, KZ, RU, TJ, TM), European (AL, AT, BE, BG, CH, CY, CZ, DE, DK, EE, ES, FI, FR, GB, GR, HR, HU, IE, IS, IT, LT, LU, LV, MC, MK, MT, NL, NO, PL, PT, RO, RS, SE, SI, SK, SM,

(54) Title: DEVICES, METHODS, AND SYSTEMS FOR DETECTION OF COLLAGEN TISSUE FEATURES

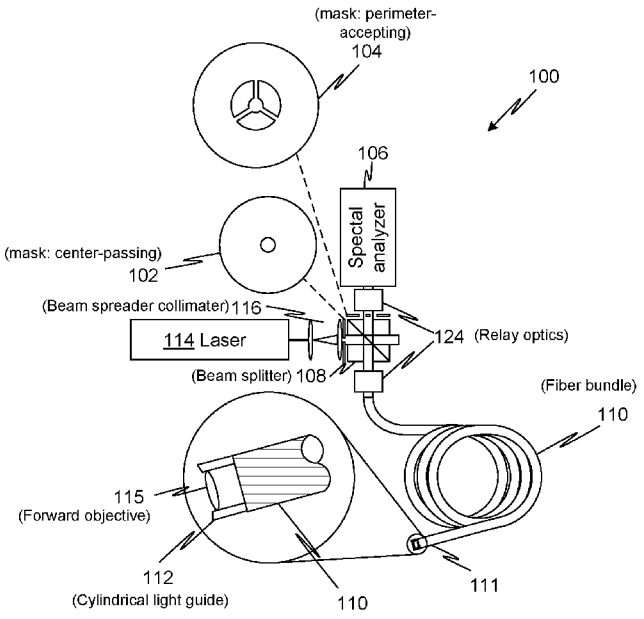


Fig. 1A

(57) Abstract: The present application discloses methods, devices, and systems for generating spatially-resolved quantification of cross-linking in cartilage based on Raman scattering of excitation light. The examples presented demonstrate that the method provides a discriminating power sufficient to distinguish early onset of osteo-arthritis even before a patient is symptomatic.

[Continued on next page]

WO 2017/214604 A1

TR), OAPI (BF, BJ, CF, CG, CI, CM, GA, GN, GQ, GW, KM, ML, MR, NE, SN, TD, TG).

Published:

— *with international search report (Art. 21(3))*
— *before the expiration of the time limit for amending the claims and to be republished in the event of receipt of amendments (Rule 48.2(h))*

Devices, Methods, And Systems for Detection of Collagen Tissue Features

CROSS REFERENCE TO RELATED APPLICATIONS

This Application claims the benefit of US Provisional Application No. 62/348,502 filed June 10, 2016, which is incorporated herein by reference in its entirety.

BACKGROUND

Osteoarthritis (OA) is a progressive joint disease that severely affects articular cartilage. OA remains asymptomatic until its late stage, when the treatment options are limited to major interventions such as joint replacement. In adults, articular cartilage is an avascular connective tissue comprised of chondrocytes and collagenous extracellular matrix (ECM). Its main function is ensuring smooth joint movement and shock absorption. The ECM structure consists predominantly of collagens (COL) and proteoglycans (PGs), with the COL matrix providing tensile strength, whereas PGs resist compression. Initiation of OA could be caused by mechanical damage (trauma), proteolytic action secondary to soft-tissue injuries, or slow, age-dependent progression. Regardless of the initiation mechanism, an imbalance in ECM homeostasis is a key pathogenic pathway of OA. This imbalance results in progressive degradation of the ECM cartilage components. The onset of OA in articular cartilage is characterized by degradation of the ECM. Specifically, breakage of cross-links between collagen fibrils in the articular cartilage leads to loss of structural integrity of the bulk tissue.

SUMMARY

The present application discloses methods, devices, and systems for generating spatially-resolved quantification of cross-linking in cartilage based on Raman scattering of excitation light. The examples presented demonstrate that the method provides a discriminating power sufficient to distinguish early onset of osteo-arthritis even before a patient is symptomatic.

Objects and advantages of embodiments of the disclosed subject matter will become apparent from the following description when considered in conjunction with the accompanying drawings.

BRIEF DESCRIPTION OF THE DRAWINGS

Objects and advantages of embodiments of the disclosed subject matter will become apparent from the following description when considered in conjunction with the accompanying drawings.

Fig. 1A shows an endoscopic detection and diagnostic instrument according to embodiments of the disclosed subject matter.

Fig. 1B shows a signal filtering and classification component of the instrument of Fig. 1A.

Fig. 1C shows a method for diagnosing arthritis in a cartilage, according to embodiments of the disclosed subject matter.

Fig. 2A is an illustration for background showing collagen fiber polymerization level assessed with atomic force microscopy.

Figs. 2B and 2C illustrate surface morphology and quantify roughness of samples used for experiments with collagen samples described herein.

Fig. 3A shows normalized Raman spectra of COL I and COL II in superposition.

Fig. 3B shows a normalized Rama spectra of control and glutaraldehyde-fixed collagen thin films.

Figs. 4A and 4B show the similarity between hydroxylysylpyridinoline, a major crosslink naturally occurring in articular cartilage and glutaraldehyde induced pyridinium-type crosslink schematic diagrams of hydroxylysylpyridinoline Fig. 4A and pyridinium-type crosslinks Fig. 4B. Central chemical compound in both crosslinks is pyridine ring.

Fig. 4C is a Raman spectrum of pyridine.

Figs. 5A and 5B show decomposition modeling of segments of COL I Raman spectrum where Fig. 5A corresponds to the first outline box in Fig. 3B and Fig. 5B corresponds to the second (right side) outline box in Fig. 3B.

Figs. 6A through 6H and 6J are spatially resolved spectral maps of the normalized integrated intensity (concentration) of the 1030 cm^{-1} Raman band associated with the pyridinium type cross-linking.

In Fig. 6A, two maps are shown, one for control and one for a thin film exposed to 0.05% glutaraldehyde solution for 1 hour.

In Fig. 6B, two maps are shown for a thin film exposed to 0.05% glutaraldehyde solution, the top for 1.5 hour and the bottom for 2 hours.

In Fig. 6C, three maps are shown for a thin film exposed to 0.05% glutaraldehyde solution, the top for 2.5 hours, the middle for 3 hours, and the bottom for 4 hours.

In Fig. 6D, two maps are shown, one for control and one for a thin film exposed to 0.1% glutaraldehyde solution for 1 hour.

In Fig. 6E, two maps are shown for a thin film exposed to 0.1% glutaraldehyde solution, the top for 1.5 hour and the bottom for 2 hours.

In Fig. 6F, three maps are shown for a thin film exposed to 0.1% glutaraldehyde solution, the top for 2.5 hours, the middle for 3 hours, and the bottom for 4 hours.

In Fig. 6G, two maps are shown, one for control and one for a thin film exposed to 0.2% glutaraldehyde solution for 1 hour.

In Fig. 6H, two maps are shown for a thin film exposed to 0.2% glutaraldehyde solution, the top for 1.5 hour and the bottom for 2 hours.

In Fig. 6J, three maps are shown for a thin film exposed to 0.2% glutaraldehyde solution, the top for 2.5 hours, the middle for 3 hours, and the bottom for 4 hours.

Fig. 7 shows averaged PYR-type cross-link concentrations for various concentrations of GA solutions. One way analysis of variants (ANOVA) was applied for data analysis.

Fig. 8A shows pyridinoline collagen cross-links density measured at 1030 cm^{-1} Raman band at D14 (+cortisol - β-aminopropionitrile, +cortisol + β-aminopropionitrile, - cortisol - β-aminopropionitrile, n = 16 per group and 3 different locations were tested on each sample) and D0 (n = 9 and 3 different locations were tested on each sample). Spectrum was normalized to proline peak at 857 cm^{-1}. A lower pyridinoline collagen cross-links concentration for + cortisol, + inhibitor group compared with + cortisol, - inhibitor group. *Error bar*: standard deviation. $*p < 0.01$: statistical change of pyridinoline densities.

Fig. 8B shows pyridinoline collagen cross-links density measured at 1030 cm^{-1} Raman band at D14 (n = 16 per group and 3 different locations were tested on each sample). Spectrum was normalized to proline peak at 857 cm^{-1}. A lower pyridinoline collagen cross-links concentration for + cortisol, + inhibitor group compared with + cortisol, - inhibitor group. *Error bar*: standard deviation. $*p < 0.01$: statistical change of pyridinoline densities.

DESCRIPTION OF THE PREFERRED EMBODIMENTS

The present disclosure describes a quantitative diagnostic tool for detecting OA at its early stages, which may be a prerequisite for development of an effective treatment that does not require joint replacement. Accordingly, there is a need for non-invasive, label-free tools for diagnosing OA at its early stage.

Osteoarthritis (OA) affects millions of Americans: it is a progressive, complex, multi-tissue joint disease with degenerative changes in the articular cartilage and subchondral bone (1), with a long asymptomatic early development and debilitating late stages. Late-stage treatment options are limited to major interventions, including joint replacement; none of the early treatment modalities offer conclusive relief to patients. Despite the significant research and clinical effort dedicated to OA, there are currently no broadly accepted quantitative diagnostic tools for the early stages of the disease. Diagnosis and therapeutic interventions at the early stage of OA offer the promise of preventative care that could provide significant benefits to patient's quality of life.

Collagen is the major structural protein of most connective tissues. It provides the structural support to resident cells in the form of extracellular matrix (ECM). Many types of collagen have been identified, with the five most common types being Type I (e.g., as found in skin, tendon, vascular ligature, organs, bone), Type II (e.g., as found in cartilage), Type III (reticulate), Type IV (e.g., forming basal lamina), and Type V (e.g., cell surfaces, hair and placenta).

The structural integrity and mechanical properties of collagen-based joint tissues is significantly affected by collagen cross-links (CxL), chemical compounds that both, connect COL fibrils as well as molecules within the COL. It has been reported that degradation of the COL CxLs compromises structural integrity of articular cartilage, which may be lead to onset of OA. In a model, β-aminopropionitrile (BAPN) was used to block the formation of pyridinoline (PYD) CxLs in an immature bovine articular cartilage explant model. In a cartilage explant model, levels of glucose, cortisol and insulin were controlled in a serum-free, chemically defined media to investigate the evolution of biochemical and mechanical properties of live immature bovine cartilage. In this model cartilage explants lost their

structural integrity in the absence of cortisol. The loss of structural integrity can be a result of degradation of CxLs in ECM. Therefore, the present disclosure proposes a method using Raman scattering capable of quantifying CxL concentrations in articular cartilage, which can advantageously be used to detect early onset OA.

Raman scattering is the process in which a small fraction of incoming photons, provided by a light source, inelastically collide with target molecules. As a result, the optical frequency of the outgoing photons is different from the incident photonic frequency, with the difference being equal to the vibrational energy of the scattering molecule. Raman spectroscopy allows investigation of functional groups and bonding types, providing information about the biochemical composition of tissues on a molecular level.

Raman micro-spectroscopy is a non-destructive and highly versatile analytical technique the exhibits vast potential for in vivo probing and in vitro analysis of biological tissues, especially as it does not require specimen preparation. However, the weakness of the signal, which is often masked by overwhelming fluorescence, has prevented a more widespread use of Raman scattering in the past. The use of infrared lasers as a light source, as well as advances in CCD detectors, have significantly improved the signal-to-noise ratio, enabling the use of Raman spectroscopy in probing tissues.

Analysis of Raman spectra obtained from articular cartilage has been challenging, and so far there is no generally accepted quantitative analysis for diagnosing early stages of OA. Thus, there is a need for methods of analyzing tissue for evaluating the presence of early stages of OA.

In one aspect, the present disclosure provides a method of analyzing mammal cartilage tissue, including generating a Raman spectrum of cartilage tissue; and measuring one or more Raman spectrum peaks corresponding to a cartilage crosslinking moiety. The cartilage may be articular cartilage and, in particular, the cartilage tissue may include collagen type I (COL I) or collagen type II (COL II).

In another aspect the cartilage tissue is of a patient with osteoarthritis, in particular early stage osteoarthritis.

The Raman spectrum may be generated using various Raman techniques and instruments. For example, the Raman spectrum is generated using Raman micro-

spectroscopy, selective-sampling Raman micro-spectroscopy, coherent anti-Stokes Raman spectroscopy (CARS), stimulated Raman spectroscopy (SRS), surface enhanced Raman spectroscopy (SERS), surface enhanced resonance Raman spectroscopy (SERRS), spatially offset Raman spectroscopy (SORS), surface enhanced spatially offset Raman spectroscopy (SESORS), or transmission Raman spectroscopy (TRS).

Preferably, the Raman spectrum is generated in vivo, more preferably by endoscopy or arthoscopy, and even more preferably the Raman spectrum is generated using a fiber optic Raman probe. The fiber optic Raman probe may be a handheld probe.

The crosslinking moiety may be any moiety establishing crosslinks within the collagen, preferably between collagen fibrils in the cartilage. The crosslinking moiety may contain a central pyridine ring with substituents attached that are suitable for crosslinking. Examples of crosslinks include pyridinium-type crosslinks and pyridinoline crosslinks. In a preferred embodiment, the crosslinking moiety contains a pyridinium ring or pentosidine. Preferably, the crosslinking moiety is pyridinoline (i.e., hydroxylsylylpyridinoline).

In an embodiment of the present disclosure, COL thin films were used as a simplified model of collagenous extracellular matrix found in articular cartilage. Raman spectroscopy was used to assess changes of the relative concentration of CxLs induced by glutaraldehyde fixation. To achieve this goal, a quantitative method was developed whereby the relatively complex Raman signal obtained from the collagen was decomposed into known chemical structures and their allowable vibrational modes. Each of the structures was then modeled as a mathematical function and their sum forms an optimization function that produces model of the spectra via curve fitting. Relevant information on the CxLs was then extracted from the model. Quantitatively assessing relative CxL concentrations in articular cartilage is proposed as an avenue for diagnosing early stage OA in an embodiment.

In an embodiment taking place in a clinical setting, a patient may be subjected to arthroscopy with a fiber optic Raman probe inserted into articular cartilage. A Raman spectrum is generated and analyzed for peaks corresponding to cartilage crosslinking moieties, thereby facilitating diagnosis of OA, in particular early stage OA.

Figs. 1A and 1B show features of an endoscopic instrument as an example of a diagnostic tool for distinguishing health from diseased tissue according to embodiments of

the disclosed subject matter. Fig. 1A illustrates an endoscopic tissue inspector 100 that transmits excitation light from a light source such as a laser 114 to a sample and receives and relays scattered light from the sample to a spectral analyzer 106. A probe 111 is used for delivery of excitation light and collection of a Raman signal. A fiber bundle 110 connects the probe 111 to a laser excitation source 114. The central fibers of the fiber bundle 110 convey the excitation light and perimeter fibers of the fiber bundle 110 convey received light from a sample to a spectral analyzer 106 which may contain a spectrometer (e.g., Horiba iHR320). An incisions may be made in the tissue of a patient as part of a surgical procedure or for diagnosis. The probe 111 may be inserted through the incision and positioned at one or more locations near the edge of an articular cartilage or other connective tissue to generate and receive a return light signal. A separate probe or one that is collinear with probe 111 may be used to image the scene inside the incision to guide the probe 111. In alternative embodiments multiple probes may be used, one for delivering excitation light and one for receiving light from the sample.

The spectral analyzer 106 may include a spectrometer 150 which receives light from a fiber bundle 110 and generates a digital representation of the spectrum of the received light. The latter may be applied to a spectral filter 152, for example which may notch out irrelevant portions of the spectrum, quantify certain peaks, or otherwise reduce the dimensionality of the information in the spectrum so that only predefined features (a feature vector) of the spectrum are applied to a pattern recognition module 156.The patter recogniation module 156 may be a computer running a program that distinguishes feature vectors characteristic of healthy tissue from feature vectors characteristic of diseased tissue. For example, the intensities of certain spectral peaks may indicate the quantity of features of cross-links in articular cartilage which further may discriminate arthritic from non-arthritic tissue as described below. The magnitudes of the spectral peaks and a symbol indicating a probability estimate for assigning a current sample to the class of diseased or healthy tissue may be output on a display 154. A user interface 158 may be used to program the pattern recognition module.

Light may be transmitted from a laser 114 according to embodiments disclosed in the experimental examples described above or others. The beam of the laser 114 may be

conditioned using a variety of optical devices to form a beam whose width corresponds to the diameter of a predefined fiber bundle 110. Note that, as will be evident from the further description, the fiber bundle 110 may be replaced by a pair of concentric light pipes as will be evident from the further disclosure or by two concentric fiber bundles separated by a concentric spacer. The widened beam emerging from a beam spreader 116 is masked by a pinhole 102 that passes light such that only the central fibers carry light toward a forward objective 115. The light from the pinhole 102 (note that despite the use of the term pinhole, it should be evident that the size of the hole is not restricted) passes to a beam splitter which allows the excitation light (from the laser 114 and pinhole 102) to be collinear along the fiber bundle with signal light from a sample returning along the concentric outer fibers of the fiber bundle 110. The reflected light is relayed by relay optics 124 to the end of the fiber bundle which is precisely positioned such that only the central fiber (or fiber) carry light toward the target. Excitation light is focused by a forward objective 115 (here figuratively shown as a single lens but in practice it would be a multi-element component with a high numerical aperture. Light scattered from the sample due to the excitation light is received by a cylindrical light guide 112 having a beveled surface and configured to accept light from multiple angles. The light guide 112 transmits received light to the outer fibers surrounding the central ones in the fiber bundle 110. Received light, including light from Raman scattering in the tissue sample passes through the relay optics 124 and beam splitter 108, masked by the perimeter accepting mask 104, and received by a spectrometer of the spectral analyzer 106.

Referring to Fig. 1C, in a method implemented by an embedded or host processor (See Figs. 1A, 1B), a cartilage is scanned as described above to acquire Raman samples at one or more locations of the cartilage. S1. A raw input vector may be generated that includes the raw Raman signal and other data such as patient record data including other conditions or diseases of the patient. S2. A reduced input vector may be constructed by filtering the Raman samples, for example, detecting magnitudes of one or more spectral peaks. S3. From the reduced Raman data, at S4, the degree of cross-linking may be quantified. In embodiments, the magnitude of cross-linking may show a distribution of magnitudes. At S5, the reduced input vector is applied to a classifier. At S6, a class is output as a diagnosis along with a

reliability estimate. The classifier may be a software implementation that is as simple as thresholding an average magnitude of Raman spectral peak(s) or a more sophisticated model that takes account of the distribution of the magnitudes of cross-linking. At S7, the class is output and spatially-resolved cross-linking maps may be output. At S8, the diagnosis may be output on a display.

EXAMPLES

Sample preparation

In an embodiment, neutralized collagen solution (PH 7.4) was prepared from 3.1 mg/ml type I collagen from bovine hides (PureCol, Advanced Biomatrix San Diego, CA, USA) in 10× Dulbecco's phosphate buffered saline (DPBS) and 0.1 M NaOH. Neutralized COL solutions were applied on alkanethiol treated gold-coated silicon wafers to produce thin films. Before being used to prepare thin films, the substrates were cut into 15 mm × 15mm pieces and placed in petri dishes. Silicon substrates were coated with a 5 nm layer of chromium and 18 nm layer of gold through thermal deposition (Edwards BOC/Auto 306 Thermal Evaporator) and rinsed with ethanol. Coating was introduced to reduce fluorescence background to the Raman spectra. 1.8 ml of the neutralized COL solution was applied onto a coated silicon wafer in a petri dish and then incubated at 37°C for 12 h.

After incubation, the samples were immersed in 1-hexadecanethiol (0.5 mM; Sigma Aldrich) ethanol solution for 8 h prior to being rinsed with ethanol and dried with filtered N_2. Incubated collagen was rinsed with 1× DPBS and deionized H_2O 10 times to remove the bulk salt and gels from the surface. After rinsing, specimens were immediately placed in DPBS (1×) and stored at 4 °C. Prior to treatment/characterization, samples were taken out of the DPBS, rinsed with deionized H_2O and dried with a filtered nitrogen gun.

The degree of fiber polymerization of thin films was assessed via atomic force microscopy (PSIA XE-100 AFM (Park Systems, Santa Clara, California, USA), whereas thickness and surface uniformity were characterized with optical profilometer. See Figs. 2A-2C.

Glutaraldehyde (GA) solution, being a known cross-linker was used to introduce various levels of collagen cross-links. Varying exposure and concentration of GA solution

controlled CxL concentration levels. Three batches of samples were treated with GA concentrations of 0.05%, 0.1% and 0.2%, respectively. There were seven samples within each batch, fixation times were 1h, 1.5h, 2h, 2.5h, 3h and 4h. 5ml of GA solution was applied onto each sample. After the fixation cross-linked COL films were rinsed with deionized water and desorbed into 20ml PBS (0.2 M, PH 7.4, Sigma Aldrich) for 48-72h. Subsequently, specimens were rinsed with deionized H_2O and DPBS (1×) several times, stored in DPBS(1×) at 4 °C and kept sterile. Cross-linked COL thin films were rinsed with deionized H_2O prior to Raman characterization.

Raman characterization

Raman spectra were acquired with a confocal micro-spectrometer (InVia, Renishaw Wotton-under-Edge, Gloucestershire, UK). Incident laser excitation was provided by helium-neon laser with 632.8 nm wavelength, delivered by 100× objective. Spectral resolution provided by 1800 gr/mm diffraction grating was 1 cm^{-1}.

Raman signal was acquired with 10 accumulations, each lasting 10 s. Prior to the acquisition of the spectrum at each measurement point, photobleaching was applied for 10 s to reduce the fluorescence background. Spatially resolved characterization was performed to generate spectral maps. A 57 mm × 30 mm window within each sample was assessed and each spectral map included 220 measurement points.

Computational implementation of the proposed model was carried in MatLab (Mathworks, Inc) as a two-step process, each requiring curve fitting of experimental data. First, the signal was pre-processed to remove fluorescence background and then relevant segments of Raman spectra were modeled. Fluorescence is commonly removed by fitting the region of the spectra below distinctive Raman bands with low order polynomial function. Fluorescence was iteratively fitted with a fifth order polynomial and subsequently subtracted from the raw signal. In the second step, the vibrational modes of interest were approximated as a damped harmonic oscillator driven by a force whose profile follows a sinusoidal curve. According to the hydrodynamic theory, Raman lines naturally follow a Lorentzian profile. Thus, the optimization function is the sum of Lorentzians. The trust region optimization model was employed for curve fitting of the Raman spectra. Conceptually, it is a maximum neighborhood method developed through interpolation between the Taylor series method and

the gradient descent method. It sets a problem as the iterative solving of a set of nonlinear algebraic equations. However, if the initial estimate is too far from the optimum, the algorithm will not converge. Therefore, the subset of the region of the objective function is defined and optimized first. The function is approximated with a simpler one which reasonably reflects the behavior of the original function in a neighborhood E around the point x. This neighborhood is referred to as the trust region. In essence, the trust region represents constraints derived from the underlying biochemistry of the specimen.

Collagen in the ECM of articular cartilage is predominantly type II (COL II), whereas due to practical considerations the present model use type I (COL I). The major difference between COL I and COL II is a "phase shift" in their chains. In COL I the NH groups point counter-clockwise when viewed from the carboxyl ends of the chains, whereas in COL II the opposite is true. If an existing set of hydrogen bonds in COL I is broken, and each polypeptide chain rotated about its own axis by approximately $\pi/3$, the NH group would instead be attached to the carbonyl oxygen, forming the hydrogen bond.

Consequently, Raman spectra of COL I and II are rather similar, as shown in Fig. 3A. Further, the proposed cross-link (CxL) concentration assessment relies on quantification of the concentration pyridine aromatic rings, which are centerpieces of bothpyridinium CxLs induced by GA-fixation in COL I and hydroxylysylpyridinoline (PYD) CxLs that are present in the COL II of the ECM of articular cartilage. The Raman band associated with in-plane stretching of pyridine ring is observed at the same location in the spectra of COL I and COL II (Fig. 3A) as well as in articular cartilage explants. The ring is a prominent CxL residue found in fibrillar COLs and most connective tissues, except cornea and skin.

Collagen is a large molecule comprised of three polypeptide chains, which form a right-handed triple helix. Each of the chains contains multiple regions of repeating amino acid sequences $(Gly\text{-}X\text{-}Y)_n$, where Gly is glycine and X and Y are often proline and hydroxyproline.

Fig. 3B depicts Raman spectra of collagen type I (COL I) obtained from a thin film sample, superimposed with the spectra of GA-treated COL I. The dominant Raman band at the far right side of the spectrum, centered at $1669cm^{-1}$, is assigned to amide I and in COL I is mainly attributed to carbonyl stretching of the peptide bond in the Gly-X-Y tripeptide

sequence. Two superimposed Raman bands in the center of the signal, with peaks at 1240 cm^{-1} and 1268 cm^{-1}, respectively represent coupling of CN stretching with NH in-plane deformation, and are assigned to amide III. The peak at 1240 cm^{-1} is associated with proline rich regions, whereas 1268 cm^{-1} corresponds to proline poor regions, respectively. Amide I and amide III, together with C-C stretching of the backbone formed by the Gly-X-Y sequence found at 935 cm^{-1}, suggest an α-helix conformation. Vibrations of the proline ring, specifically C-C stretching, is attributed to Raman bands centered at 853 cm^{-1} and 918 cm^{-1}, and the hydroxyproline ring gives rise to Raman band with peak at 875 cm^{-1}. The isolated Raman band located at 1030 cm-1 is associated with C-C stretching of aromatic pyridine ring.

In an embodiment, GA treatment resulted in a shift of the amide I and amide III bands. The peak of the amide I bandshifted to 1674 cm^{-1}, and bands attributed to Amide III became centered at 1235 cm^{-1} and 1264 cm^{-1}, respectively. In the spectra of GA-fixed samples, a new band appeared at 865 cm^{-1} which is attributed to COC symmetric stretching. This band is due to ether-type COC CxL, which is a result of the reaction of the GA aldehyde group with the carbonyl group of the peptide bond in COL. Newly formed ether-type bond weakens hydrogen bonds, producing conformational modifications of the protein structure, which are seen as Raman shifts of the amide I and amide III bands. Quaternary pyridinium compounds form stable CxLs in GA-fixed samples. The 1030 cm^{-1} band is due to in-plane deformation of six-membered aromatic ring and is an indicator of the 1, 3, 5- substituted pyridine ring, similar to the CxLs of interest in articular COL .

Pyridinium-type CxLs in GA-fixed COL samples have a pyridine ring as their central feature whose vibrational modes are similar to monosubstituted six-membered rings. Similarly PYD, which is one of the major COL CxLs and is responsible for the tensile strength and structural integrity of cartilage ECM has a pyridine-like aromatic ring as its central chemical structure (Figs. 4A and 4B). Assessment of relative concentration of pyridine rings in articular cartilage thus can provide information about the concentration of PYR CxLs. Stable vibrational modes of pyridine consist of in-plane ring deformation and symmetric ring breathing modes as shown in Fig. 4C. The former involves displacing alternate carbon atoms around the ring and is characterized by a rise of the 1030 cm^{-1} band.

The latter is attributed to symmetric ring stretching that involves all carbons and nitrogen moving in and out in unison. The Raman band associated with this mode is located at 992 cm^{-1}. The 1030 cm^{-1} band is present in both purified COL (box II in Fig. 3B) and bovine articular cartilage explants. Furthermore, there is no significant overlapping of the Raman band centered at 1030 cm^{-1} and other bands in the COL spectra, which simplifies the analysis to some extent.

Quantification of the changes in the relative concentration of pyridinium-type CxLs was achieved via modeling of the experimental data, which enabled the analysis of changes in individual Raman bands due to GA-fixation. It is assumed that the relative concentration of the pyridine rings within the focal volume is proportional to the normalized integrated intensity of the Raman band associated with in-plane ring deformation. Modeling of the spectrum was needed to assess contributions of the individual bands to the complex signal that is comprised of a relatively large number of overlapping Raman bands.

Subsequently, quantitative information about the particular Raman band of interest could be extracted from the model. By taking advantage of the additive property of the Raman signal, segments of interest in the COL Raman spectra (box I and box II in Fig. 3B) can be seen as the sum of the individual bands. Therefore, the optimization function, which is used to model the spectrum, is the sum of the functions describing individual bands. The concentration of CxLs is quantified as the area under the curve of the 1030 cm^{-1} peak in the modeled spectrum, normalized by the area under the hydroxyproline curve assigned to COL. Normalization can help avoid errors which could arise as a result of concentration-dependent changes. The trust region optimization model used for these analyses, is an adaptive method that utilizes a two-step approach in which the approximation model predicts the improvement of the system being optimized before resorting to a detailed model that confirms the validity of the initial approximation, followed by constrained variation of the trust region. The modeling may include a locally constrained optimal step in the otherwise unconstrained approximate iteration. The underlying biochemistry, including the location of the peak assignments, helped to introduce appropriate constraints in the optimization model so that a unique solution could be obtained.

This approach yields a unique solution when treating large numbers of varying parameters, while being sufficiently sensitive to capture subtle changes in the vibrational spectra that arise from the potentially modest changes in the crosslink density. Two segments of the spectrum have been modeled, and the resulting modeled spectrum closely matches experimental data shown in Figs. 5A and 5B. From the first segment the integrated intensity of the hydroxyproline band has been extracted and used to normalize the integrated intensity of the band centered at 1030cm^{-1}, which is associated with in-plane stretching of pyridine rings.

Spatially resolved characterization of the COL thin films was utilized for generation of spectral maps shown in the non-limiting example of Figs. 6A through 6J. Each spectrum in the map was modeled as outlined above and the integrated intensity of the 1030 cm^{-1} band was utilized as a parameter that represents CxL relative concentration. Each map depicted in Figs. 6A through 6J corresponds to a specimen subjected to GA fixation. It can be seen that an increase in the concentration of GA and prolonged exposure to GA both produce an increase in the relative concentration of pyridinium-type CxLs.

Averaged values of CxL concentrations at different exposure times and GA concentrations are summarized in Fig. 7. COL thin films exposed to 0.05% GA experience a nearly linear increase in the relative CxL concentration, whereas specimens treated with 0.1 % and 0.2% GA solution exhibit a higher rate of increase in the first hour of exposure, after which the increase rate slows down and becomes similar to that seen in samples fixed with 0.05% GA solution.

A collagen thin film model to simulate changes in relative crosslink concentration in extracellular matrix of an articular cartilage has been introduced. Samples were treated with varying concentrations of glutaraldehyde solutions at different exposure times to induce pyridinium-type crosslinks. These crosslinks are relevant to this model system as their centerpiece is the pyridine ring, which is also the central chemical feature of hydroxylysyl pyridinoline. Hydroxylysyl pyridinoline is a crosslink found in the extracellular matrix of articular cartilage, and its degradation is associated with loss of cartilage structural stability.

Clinical model (cartilage explant model)

In this model, β-aminopropionitrile (BAPN) was used as inhibitor blocking formation of pyridinoline (PYD) CxLs in an immature bovine articular cartilage explant model. In a cartilage explant model, levels of glucose, cortisol and insulin were controlled in a serum-free, chemically defined media to investigate the evolution of biochemical and mechanical properties of live immature bovine cartilage. It was determined that the presence of BAPN and the absence of cortisol each reduced PYD concentration, corresponding to loss of structural integrity of the cartilage.

72 samples were obtained from 4 joints divided into 4 groups, n = 20 per group (n = 5 from each joint) for +BAPN, -BAPN and -cortisol groups, n =12 for day 0 group.

For Raman characterization, n = 16 were tested for +BAPN, -BAPN and -cortisol groups, and n = 9 were tested for day 0 group on day 14. For each sample, 3 different spots were characterized. Therefore, 48 spectra were characterized for +BAPN, -BAPN and -cortisol groups and 27 spectra were characterized for the day 0 group.

Results are shown in Figs. 8A and 8B. Fig. 8A and 8B both show lower PYD CxLs concentration for + cortisol, + inhibitor group compared with + cortisol, - inhibitor group (the error bar shows standard deviation; *$p < 0.01$: statistical change of PYD densities).

Fig. 8A shows PYD CxLs density measured at 1030 cm^{-1} Raman band at D14 (+cortisol -BAPN, +cortisol +BAPN, -cortisol -BAPN, n = 16 per group and 3 different locations were tested on each sample) and D0 (n = 9 and 3 different locations were tested on each sample). The spectrum was normalized to proline peak at 857 cm^{-1}. A lower PYD CxLs concentration for + cortisol, + inhibitor group compared with + cortisol, - inhibitor group. Fig. 8B shows PYD CxLs density measured at 1030 cm-1 Raman band at D14 (n = 16 per group and 3 different locations were tested on each sample). The spectrum was normalized to proline peak at 857 cm-1. Lower PYD CxLs concentration was found for +cortisol, +inhibitor group compared with +cortisol, -inhibitor group.

According to embodiments, the disclosed subject matter includes a method of analyzing mammal cartilage tissue. The method includes generating a Raman spectrum of cartilage tissue. The method further includes measuring one or more Raman spectrum peaks corresponding to a cartilage crosslinking moiety.

In embodiments, the cartilage may be articular cartilage. The articular cartilage may include collagen type I or collagen type II. The cartilage tissue may be of a patient with early stage osteoarthritis. The Raman spectrum may be generated using Raman micro-spectroscopy, selective-sampling Raman micro-spectroscopy, coherent anti-Stokes Raman spectroscopy (CARS), stimulated Raman spectroscopy (SRS), surface enhanced Raman spectroscopy (SERS), spatially offset Raman spectroscopy (SORS), surface enhanced spatially offset Raman spectroscopy (SESORS), or transmission Raman spectroscopy (TRS). The Raman spectrum may be generated in vivo. The Raman spectrum may be generated by endoscopy or arthoscopy. The Raman spectrum may be generated using an arthroscope. The Raman spectrum may be generated using a fiber optic Raman probe. The fiber optic Raman probe may be a handheld probe. The crosslinking moiety may contain a pyridinium ring or pentosidine. The crosslinking moiety may be hydroxylsylylpyridinoline.

According to further embodiments, the disclosed subject matter includes a method of analyzing Raman spectral data from collagen. The method includes decomposing a Raman signal from the collagen into predetermined chemical structures and their respective allowable vibrational modes. The method further includes modeling each of said predetermined chemical structures as a mathematical function. The method further includes combining the mathematical functions into an optimization function that produces a model of the spectra. The method further includes extracting information from the model indicative of changes in relative concentration of CxLs and quantitatively assessing changes in relative concentration of CxLs induced by glutaraldehyde fixation to diagnose the osteoarthritis.

In further variations of the foregoing method, the collagen is obtained from articular cartilage. In further embodiments of the foregoing method, the Raman spectral data is obtained using a confocal micro-spectrometer. In further embodiments of the foregoing method, the combining step includes curve fitting to produce the model of the spectra. In further embodiments of the foregoing method, the combining step includes iteratively fitting a fifth order polynomial and subtracting the fifth order polynomial from a raw signal of fluorescence.

According to still further embodiments, the disclosed subject matter includes a method of diagnosing osteoarthritis. The method includes decomposing a Raman signal from

collagen into predetermined chemical structures and their respective allowable vibrational modes. The method further includes modeling each of said predetermined chemical structures as a mathematical function. The method further includes combining the mathematical functions into an optimization function that produces a model of the spectra. The method further includes extracting information from the model indicative of changes in relative concentration of CxLs. The method further includes quantitatively assessing changes in relative concentration of CxLs induced by glutaraldehyde fixation to diagnose the osteoarthritis.

In further variations of the foregoing methods, methods may include applying the Raman signal to cartilage in a joint or acquiring Raman spectra with a confocal micro-spectrometer.

The combining may include curve-fitting to produce the model of the spectra. The combining may include iteratively fitting a fifth order polynomial and subtracting the fifth order polynomial from a raw signal of fluorescence.

According to further embodiments, the disclosed subject matter includes a method of diagnosing osteoarthritis. The method may include scanning a cartilage at multiple locations of the cartilage to obtain Raman signal from each of the locations. The method may further include quantifying cross-linking in the cartilage responsively to said signal for each location. The method may further include generating a display of spatially-resolved magnitudes of cross-linking responsively to said quantifying.

The quantifying may include detecting magnitudes of peaks of a spectrum for each of said locations. The method may include classifying said cartilage according to a degree of osteoarthritis.

According to further embodiments, the disclosed subject matter includes a system for diagnosing osteoarthritis. An optical probe is configured to deliver excitation light and receive signal light responsively to Raman scattering resulting from illumination by said excitation light. A spectral analyzer is connected to the probe to receive said signal light and to generate reduced spectral data from a spectrum thereof. A machine classifier is programmed to distinguish between healthy and arthritic cartilage from said reduced spectral data and to output an indication responsive to a detected class.

The reduced spectral data may include a magnitude of at least one spectral peak. The reduced spectral data may include a magnitude of multiple spectral peaks. The reduced spectral data may include a magnitude of at least one spectral peak at each of multiple locations within a target sample.

The foregoing descriptions apply, in some cases, to examples generated in a laboratory, but these examples can be extended to production techniques. For example, where quantities and techniques apply to the laboratory examples, they should not be understood as limiting.

Features of the disclosed embodiments may be combined, rearranged, omitted, etc., within the scope of the invention to produce additional embodiments. Furthermore, certain features may sometimes be used to advantage without a corresponding use of other features.

It is, thus, apparent that there is provided, in accordance with the present disclosure, devices methods and systems for detecting features of collagen containing tissues and by way of example, particularly, for diagnosing osteoarthritis. Many alternatives, modifications, and variations are enabled by the present disclosure. While specific embodiments have been shown and described in detail to illustrate the application of the principles of the invention, it will be understood that the invention may be embodied otherwise without departing from such principles. Accordingly, Applicants intend to embrace all such alternatives, modifications, equivalents, and variations that are within the spirit and scope of the present invention.

It will be appreciated that the modules, processes, systems, and sections described above can be implemented in hardware, hardware programmed by software, software instruction stored on a non-transitory computer readable medium or a combination of the above. For example, a method for classifying Rama spectral data can be implemented, for example, using a processor configured to execute a sequence of programmed instructions stored on a non-transitory computer readable medium. For example, the processor can include, but not be limited to, a personal computer or workstation or other such computing system that includes a processor, microprocessor, microcontroller device, or is comprised of control logic including integrated circuits such as, for example, an Application Specific Integrated Circuit (ASIC). The instructions can be compiled from source code instructions

provided in accordance with a programming language such as Java, C++, C#.net or the like. The instructions can also comprise code and data objects provided in accordance with, for example, the Visual Basic™ language, LabVIEW, or another structured or object-oriented programming language. The sequence of programmed instructions and data associated therewith can be stored in a non-transitory computer-readable medium such as a computer memory or storage device which may be any suitable memory apparatus, such as, but not limited to read-only memory (ROM), programmable read-only memory (PROM), electrically erasable programmable read-only memory (EEPROM), random-access memory (RAM), flash memory, disk drive and the like.

Furthermore, the modules, processes, systems, and sections can be implemented as a single processor or as a distributed processor. Further, it should be appreciated that the steps mentioned above may be performed on a single or distributed processor (single and/or multi-core). Also, the processes, modules, and sub-modules described in the various figures of and for embodiments above may be distributed across multiple computers or systems or may be co-located in a single processor or system. Exemplary structural embodiment alternatives suitable for implementing the modules, sections, systems, means, or processes described herein are provided below.

The modules, processors or systems described above can be implemented as a programmed general purpose computer, an electronic device programmed with microcode, a hard-wired analog logic circuit, software stored on a computer-readable medium or signal, an optical computing device, a networked system of electronic and/or optical devices, a special purpose computing device, an integrated circuit device, a semiconductor chip, and a software module or object stored on a computer-readable medium or signal, for example.

Embodiments of the method and system (or their sub-components or modules), may be implemented on a general-purpose computer, a special-purpose computer, a programmed microprocessor or microcontroller and peripheral integrated circuit element, an ASIC or other integrated circuit, a digital signal processor, a hardwired electronic or logic circuit such as a discrete element circuit, a programmed logic circuit such as a programmable logic device (PLD), programmable logic array (PLA), field-programmable gate array (FPGA), programmable array logic (PAL) device, or the like. In general, any process capable of

implementing the functions or steps described herein can be used to implement embodiments of the method, system, or a computer program product (software program stored on a non-transitory computer readable medium).

Furthermore, embodiments of the disclosed method, system, and computer program product may be readily implemented, fully or partially, in software using, for example, object or object-oriented software development environments that provide portable source code that can be used on a variety of computer platforms. Alternatively, embodiments of the disclosed method, system, and computer program product can be implemented partially or fully in hardware using, for example, standard logic circuits or a very-large-scale integration (VLSI) design. Other hardware or software can be used to implement embodiments depending on the speed and/or efficiency requirements of the systems, the particular function, and/or particular software or hardware system, microprocessor, or microcomputer being utilized. Embodiments of the method, system, and computer program product can be implemented in hardware and/or software using any known or later developed systems or structures, devices and/or software by those of ordinary skill in the applicable art from the function description provided herein and with a general basic knowledge of machine classification and signal analysis and/or computer programming arts.

Moreover, embodiments of the disclosed method, system, and computer program product can be implemented in software executed on a programmed general purpose computer, a special purpose computer, a microprocessor, or the like.

The presently disclosed subject matter is not intended to be limited to the specific embodiments disclosed above. Although the foregoing subject matter has been described in some detail by way of illustration and example for purposes of clarity of understanding, the description above is not meant to be limiting, and those skilled in the art will understand that certain changes and modifications can be practiced within the scope of the claims. Thus, modifications and other embodiments are intended to be included within the scope of the appended claims.

CLAIMS

1. A method of analyzing mammal cartilage tissue, comprising:

generating a Raman spectrum of cartilage tissue; and

measuring one or more Raman spectrum peaks corresponding to a cartilage crosslinking moiety.

2. The method of claim 1, wherein the cartilage is articular cartilage.

3. The method of claim 2, wherein the articular cartilage comprises collagen type I or collagen type II.

4. The method of claim 1, wherein the cartilage tissue is of a patient with early stage osteoarthritis.

5. The method of claim 1, wherein the Raman spectrum is generated using Raman micro-spectroscopy, selective-sampling Raman micro-spectroscopy, coherent anti-Stokes Raman spectroscopy (CARS), stimulated Raman spectroscopy (SRS), surface enhanced Raman spectroscopy (SERS), spatially offset Raman spectroscopy (SORS), surface enhanced spatially offset Raman spectroscopy (SESORS), or transmission Raman spectroscopy (TRS).

6. The method of claim 1, wherein the Raman spectrum is generated in vivo.

7. The method of claim 6, wherein the Raman spectrum is generated by endoscopy or arthoscopy.

8. The method of claim 7, wherein the Raman spectrum is generated using an arthroscope.

9. The method of claim 8, wherein the Raman spectrum is generated using a fiber optic Raman probe.

10. The method of claim 9, wherein the fiber optic Raman probe is a handheld probe.

11. The method of claim 1, wherein the crosslinking moiety contains a pyridinium ring or pentosidine.

12. The method of claim 1, wherein the crosslinking moiety is hydroxylsylylpyridinoline.

13. A method of analyzing Raman spectral data from collagen, comprising:

decomposing a Raman signal from the collagen into predetermined chemical

structures and their respective allowable vibrational modes;

modeling each of said predetermined chemical structures as a mathematical function;

combining the mathematical functions into an optimization function that produces a model of the spectra;

extracting information from the model indicative of changes in relative concentration of CxLs; and

quantitatively assessing changes in relative concentration of CxLs induced by glutaraldehyde fixation to diagnose the osteoarthritis.

14. The method of claim 13, wherein the collagen is obtained from articular cartilage.

15. The method of claim 14, wherein the Raman spectral data is obtained using a confocal micro-spectrometer.

16. The method of claim 13, wherein the combining step includes curve fitting to produce the model of the spectra.

17. The method of claim 13, wherein the combining step includes iteratively fitting a fifth order polynomial and subtracting the fifth order polynomial from a raw signal of fluorescence.

18. A method of diagnosing osteoarthritis, the method comprising:

decomposing a Raman signal from collagen into predetermined chemical structures and their respective allowable vibrational modes;

modeling each of said predetermined chemical structures as a mathematical function;

combining the mathematical functions into an optimization function that produces a model of the spectra;

extracting information from the model indicative of changes in relative concentration of CxLs; and

quantitatively assessing changes in relative concentration of CxLs induced by glutaraldehyde fixation to diagnose the osteoarthritis.

19. The method according to claim 18, further comprising:

applying the Raman signal to cartilage in a joint.

20. The method according to claim 19, further comprising:

acquiring Raman spectra with a confocal micro-spectrometer.

21. The method according to claim 18, wherein

the combining step includes curve fitting to produce the model of the spectra.

22. The method according to claim 21, wherein the combining includes

iteratively fitting a fifth order polynomial and subtracting the fifth order polynomial from a raw signal of fluorescence.

23. A method of diagnosing osteoarthritis, the method comprising:

scanning a cartilage at multiple locations of the cartilage to obtain Raman signal from each of the locations;

quantifying cross-linking in the cartilage responsively to said signal for each location;

generating a display of spatially-resolved magnitudes of cross-linking responsively to said quantifying.

24. The method of claim 23, wherein the quantifying includes detecting magnitudes of peaks of a spectrum for each of said locations.

25. The method of claim 23, further comprising classifying said cartilage according to a degree of osteoarthritis.

26. A system for diagnosing osteoarthritis, comprising:

an optical probe configured to deliver excitation light and receive signal light responsively to Raman scattering resulting from illumination by said excitation light;

a spectral analyzer connected to the probe to receive said signal light and to generate reduced spectral data from a spectrum thereof;

a machine classifier programmed to distinguish between healthy and arthritic cartilage from said reduced spectral data and to output an indication responsive to a detected class.

27. The system of claim 26, wherein the reduced spectral data includes a magnitude of at least one spectral peak.

28. The system of claim 26, wherein the reduced spectral data includes a magnitude of multiple spectral peaks.

29. The system of claim 26, wherein the reduced spectral data includes a magnitude of at least one spectral peak at each of multiple locations within a target sample.

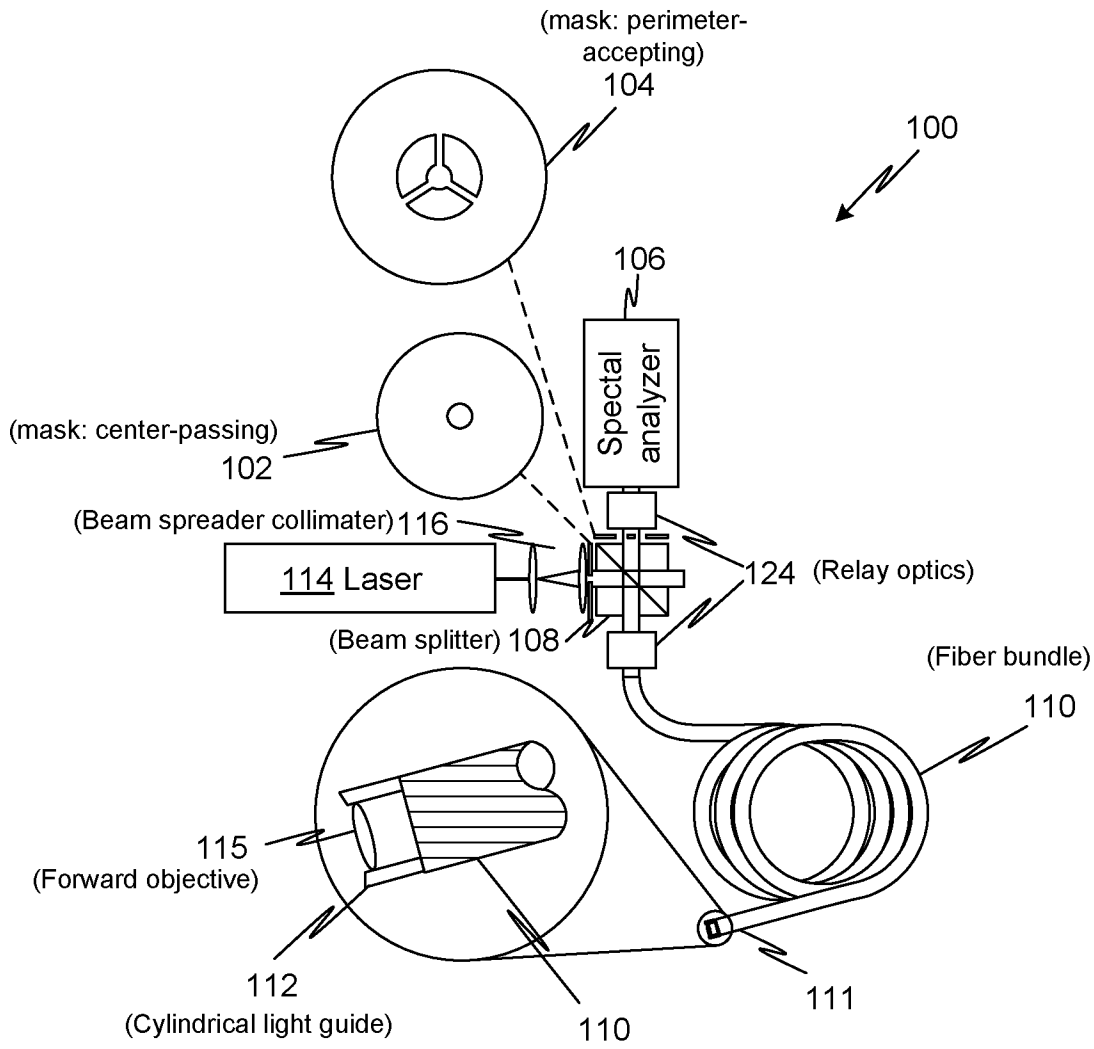

(mask: perimeter-accepting)
104
100
106
Spectal analyzer
(mask: center-passing)
102
(Beam spreader collimater) 116
114 Laser
124 (Relay optics)
(Beam splitter) 108
(Fiber bundle)
110
115
(Forward objective)
112
(Cylindrical light guide)
110
111

Fig. 1A

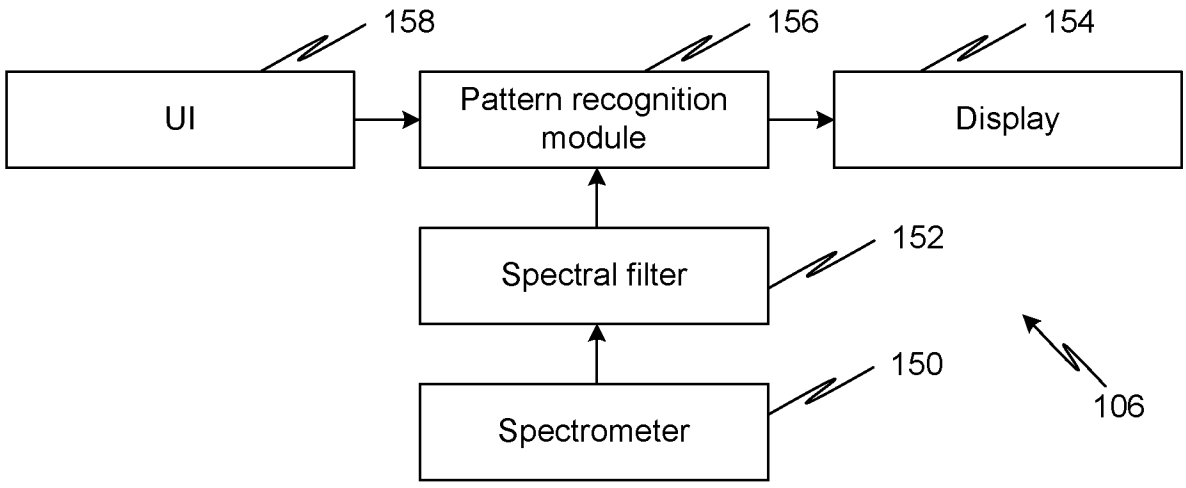

158
156
154
UI
Pattern recognition module
Display
Spectral filter
152
150
Spectrometer
106

Fig. 1B

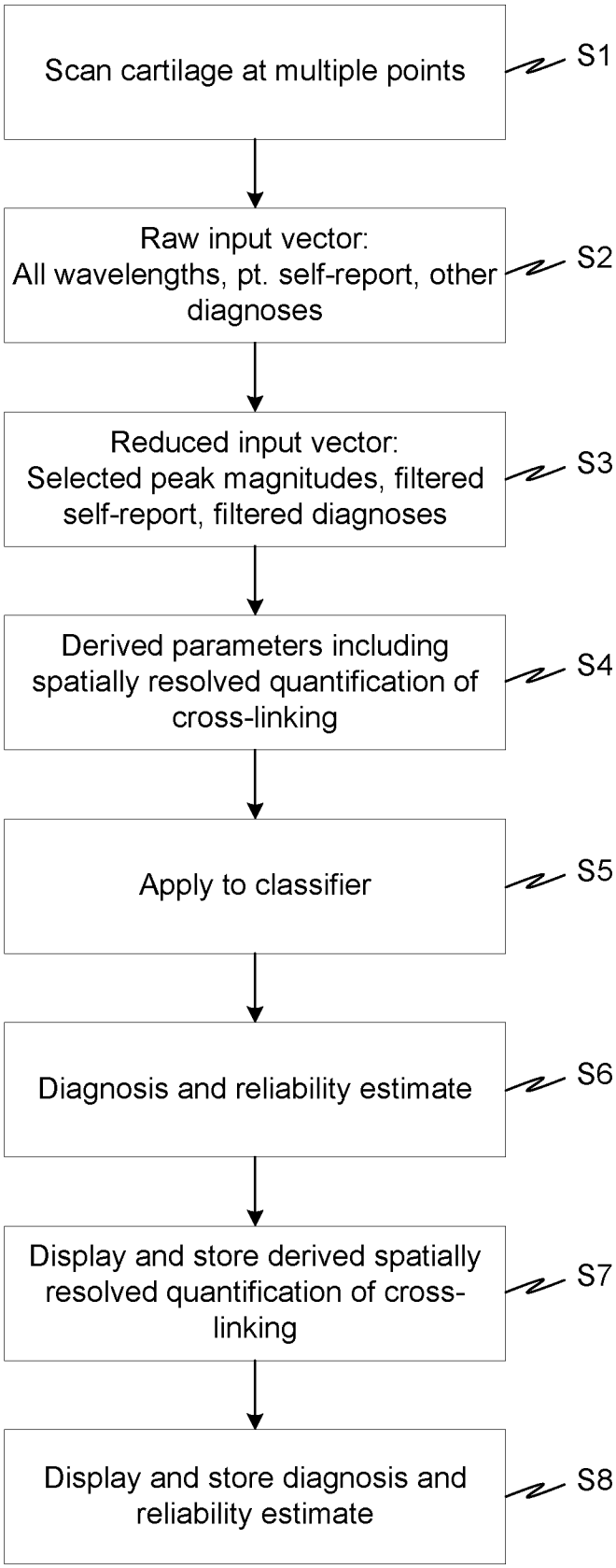

Scan cartilage at multiple points
S1
Raw input vector:
All wavelengths, pt. self-report, other diagnoses
S2
Reduced input vector:
Selected peak magnitudes, filtered self-report, filtered diagnoses
S3
Derived parameters including spatially resolved quantification of cross-linking
S4
Apply to classifier
S5
Diagnosis and reliability estimate
S6
Display and store derived spatially resolved quantification of cross-linking
S7
Display and store diagnosis and reliability estimate
S8

Fig. 1C

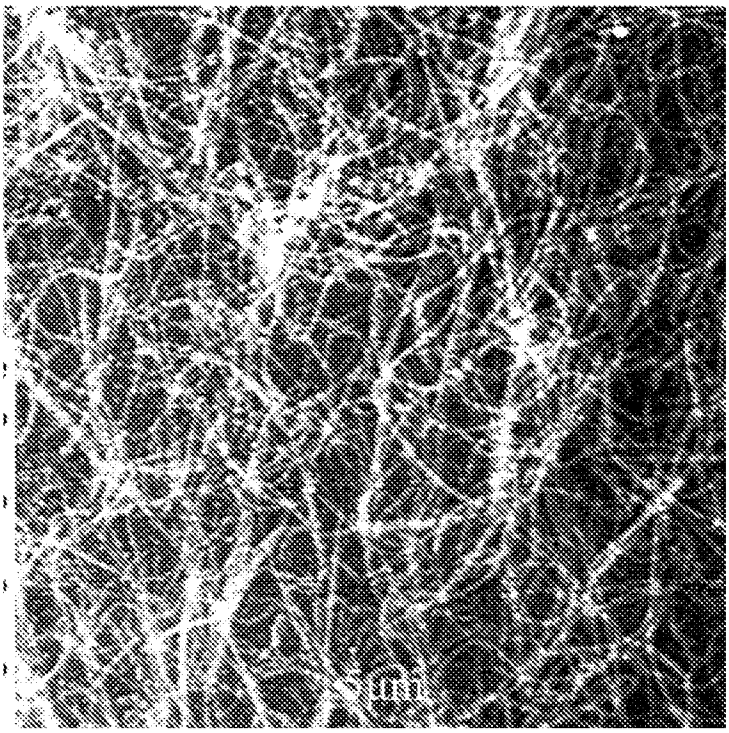


Fig. 2A

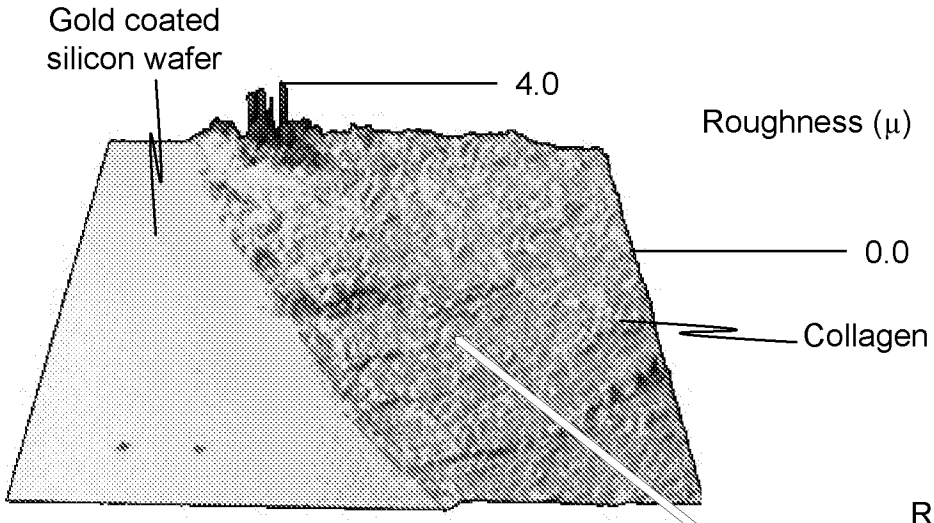


Fig. 2B

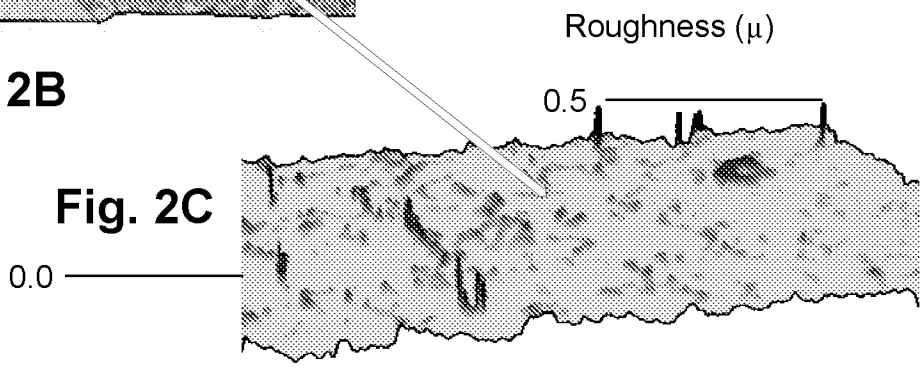


Fig. 2C

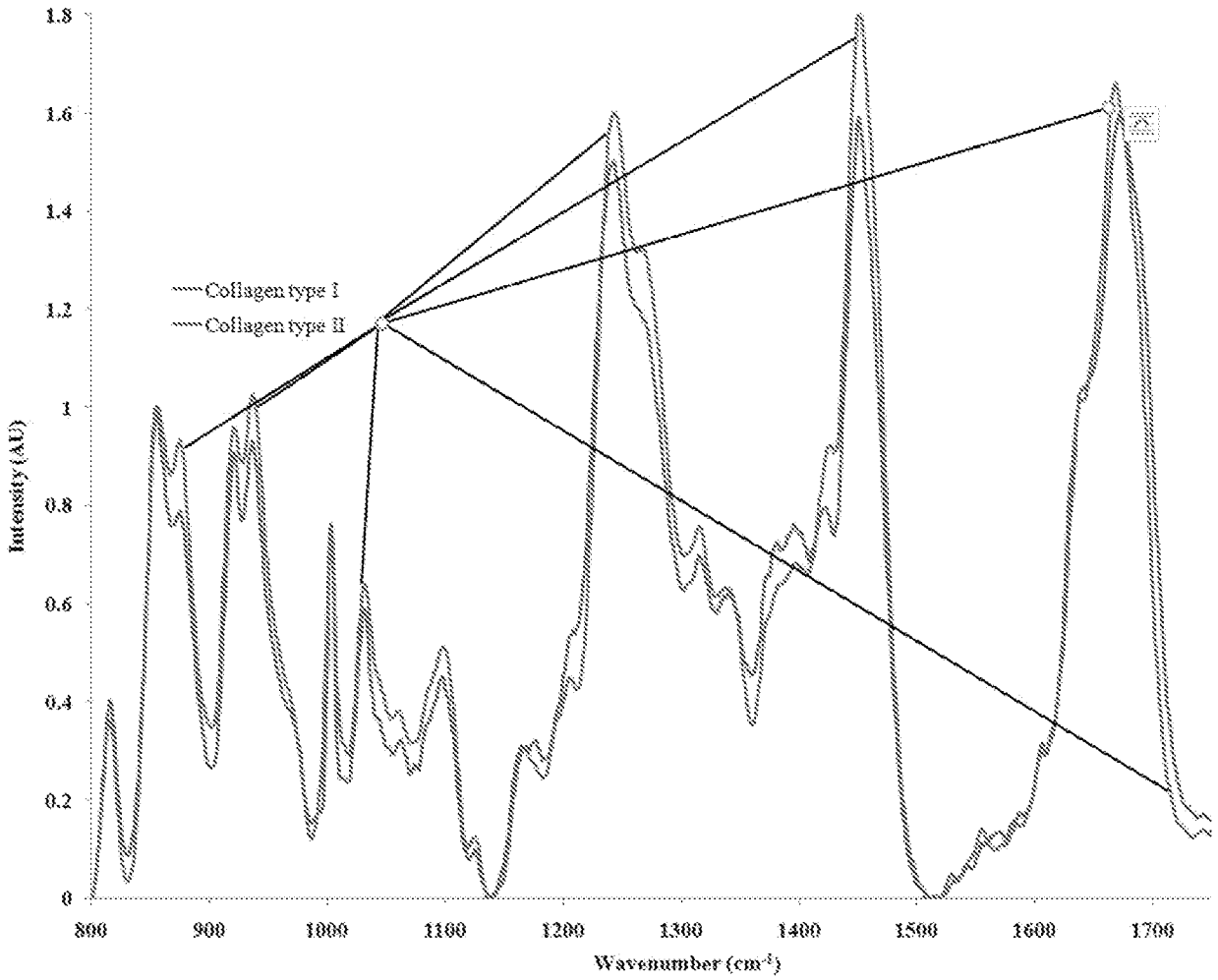

Collagen type I
Collagen type II
Intensity (AU)
Wavenumber (cm-1)
1.8
1.6
1.4
1.2
1
0.8
0.6
0.4
0.2
0
800
900
1000
1100
1200
1300
1400
1500
1600
1700

Fig. 3A

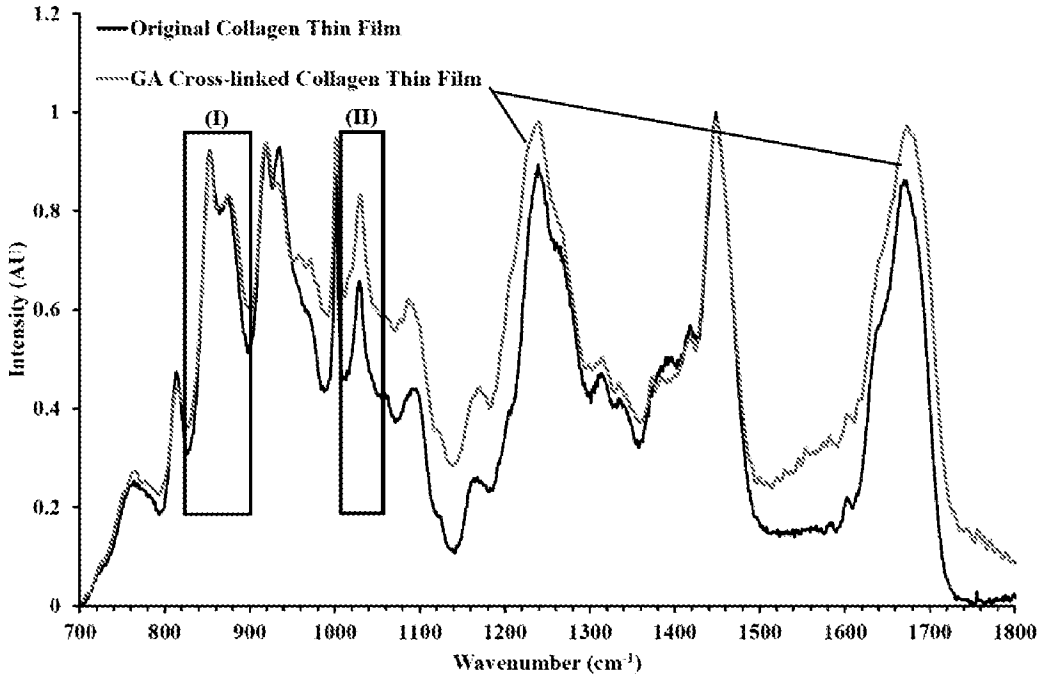
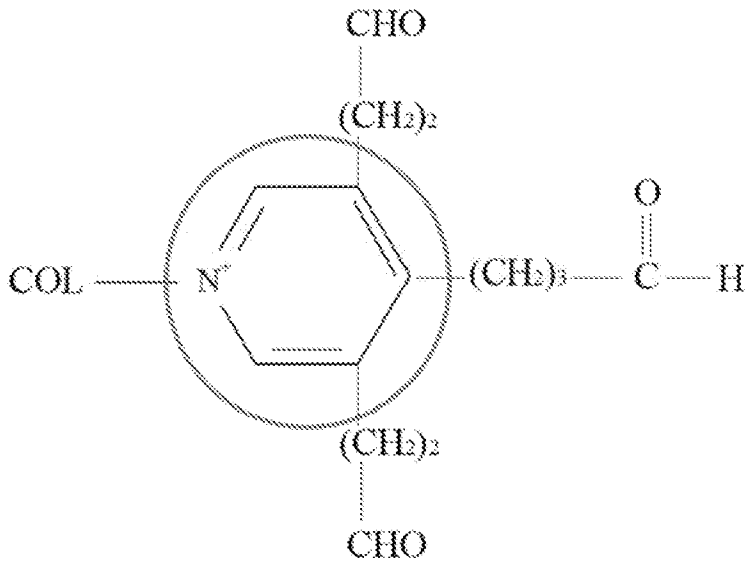
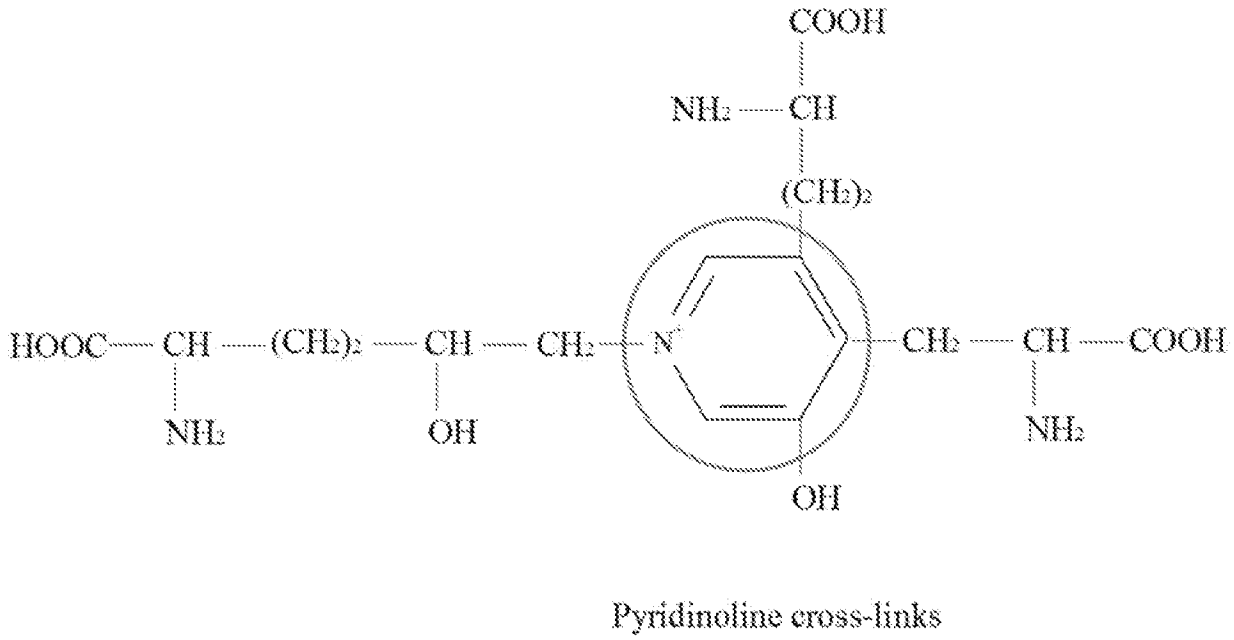


Fig. 3B



Pyridinium cross-links

Fig. 4A



Pyridinoline cross-links

Fig. 4B

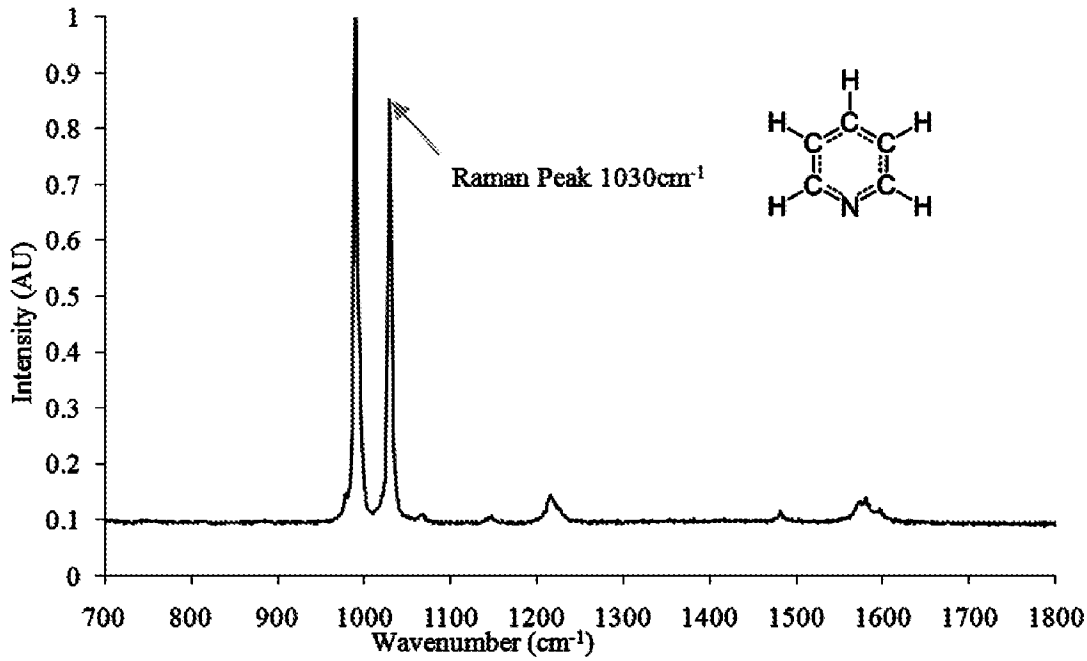


Fig. 4C

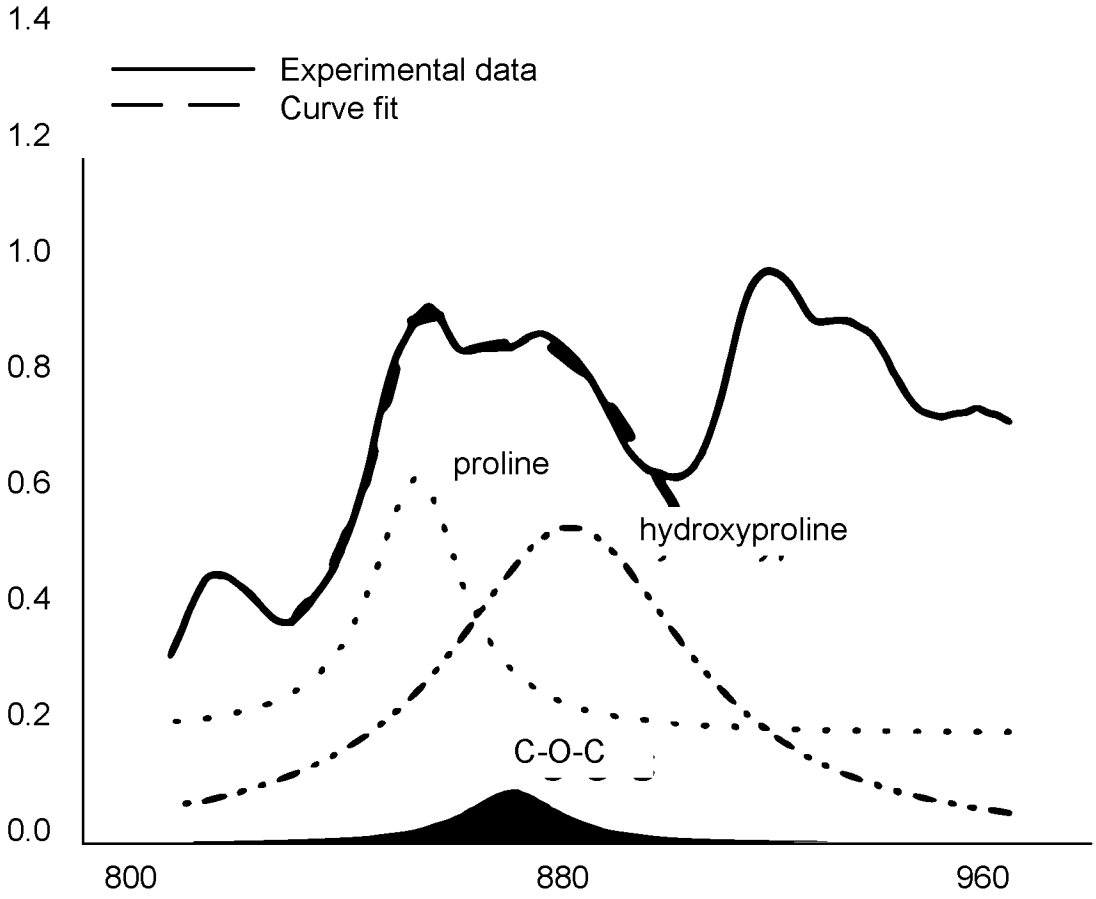

1.4
Experimental data
Curve fit
1.2
1.0
0.8
0.6
0.4
0.2
0.0
proline
hydroxyproline
C-O-C
800
880
960

Fig. 5A

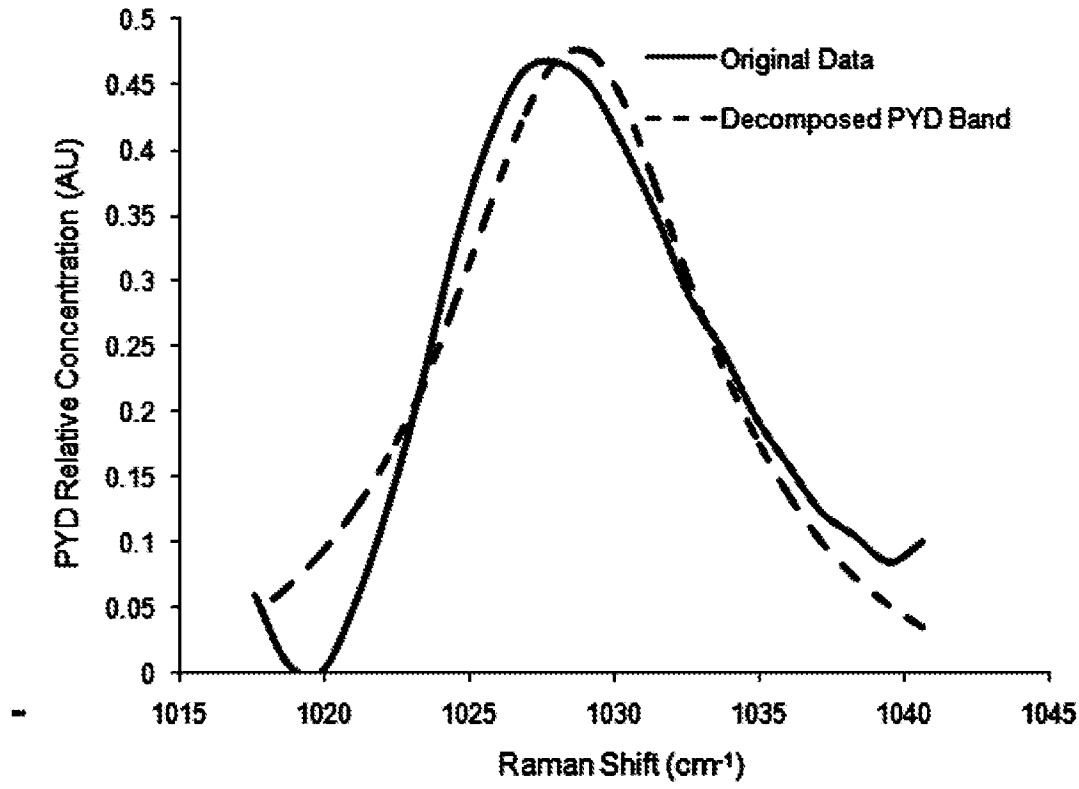

0.5
0.45
0.4
0.35
0.3
0.25
0.2
0.15
0.1
0.05
0
PYD Relative Concentration (AU)
Original Data
Decomposed PYD Band
1015
1020
1025
1030
1035
1040
1045
Raman Shift (cm-1)

Fig. 5B

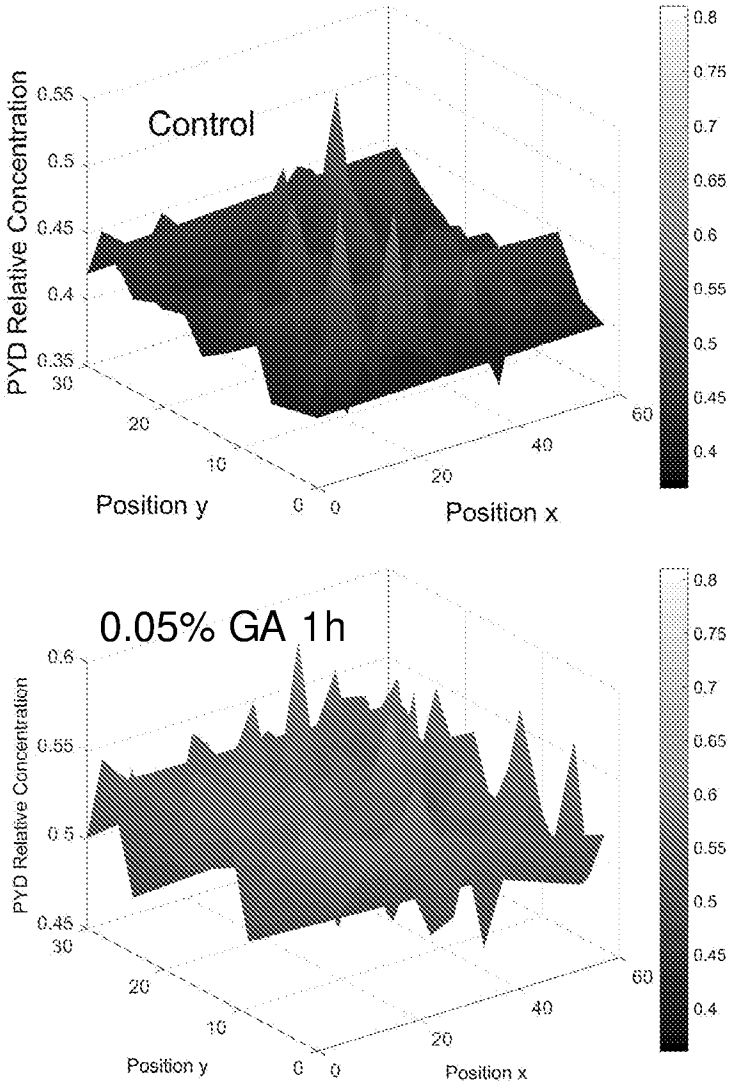

Control
PYD Relative Concentration
0.55
0.5
0.45
0.4
0.35
30
20
10
0
Position y
0
20
40
60
Position x
0.8
0.75
0.7
0.65
0.6
0.55
0.5
0.45
0.4
0.05% GA 1h
PYD Relative Concentration
0.6
0.55
0.5
0.45
30
20
10
0
Position y
0
20
40
60
Position x
0.8
0.75
0.7
0.65
0.6
0.55
0.5
0.45
0.4

Fig. 6A

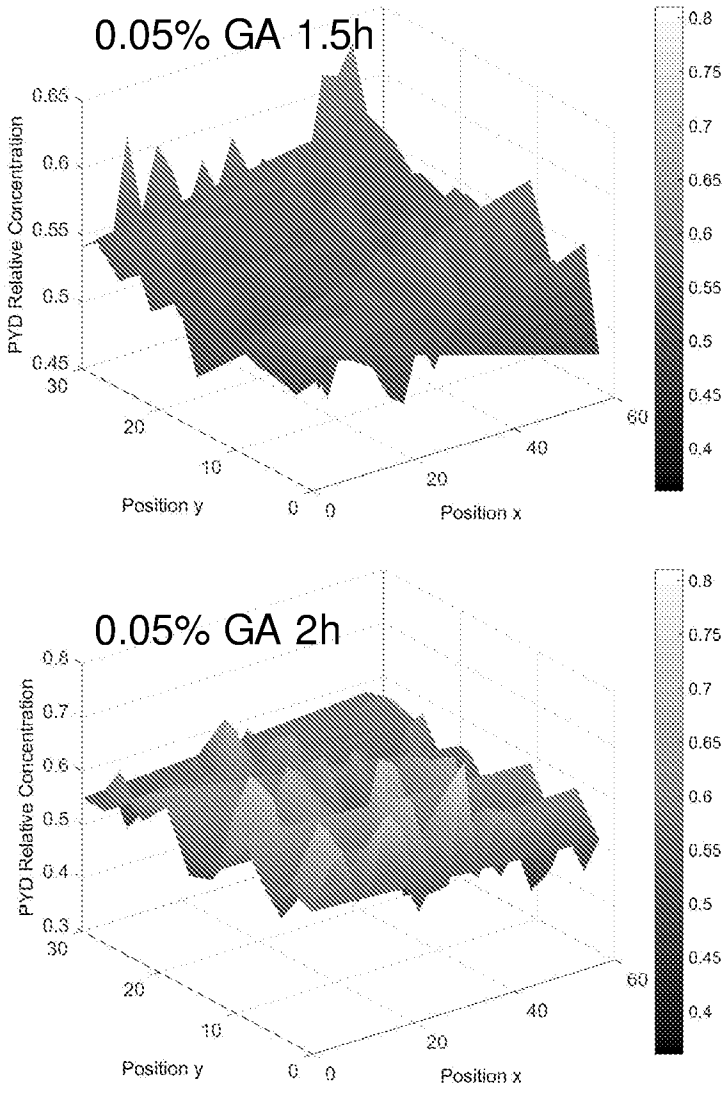

0.05% GA 1.5h
PYD Relative Concentration
0.65
0.6
0.55
0.5
0.45
30
20
10
0
Position y
0
20
40
60
Position x
0.8
0.75
0.7
0.65
0.6
0.55
0.5
0.45
0.4
0.05% GA 2h
PYD Relative Concentration
0.8
0.7
0.6
0.5
0.4
0.3
30
20
10
0
Position y
0
20
40
60
Position x
0.8
0.75
0.7
0.65
0.6
0.55
0.5
0.45
0.4

Fig. 6B

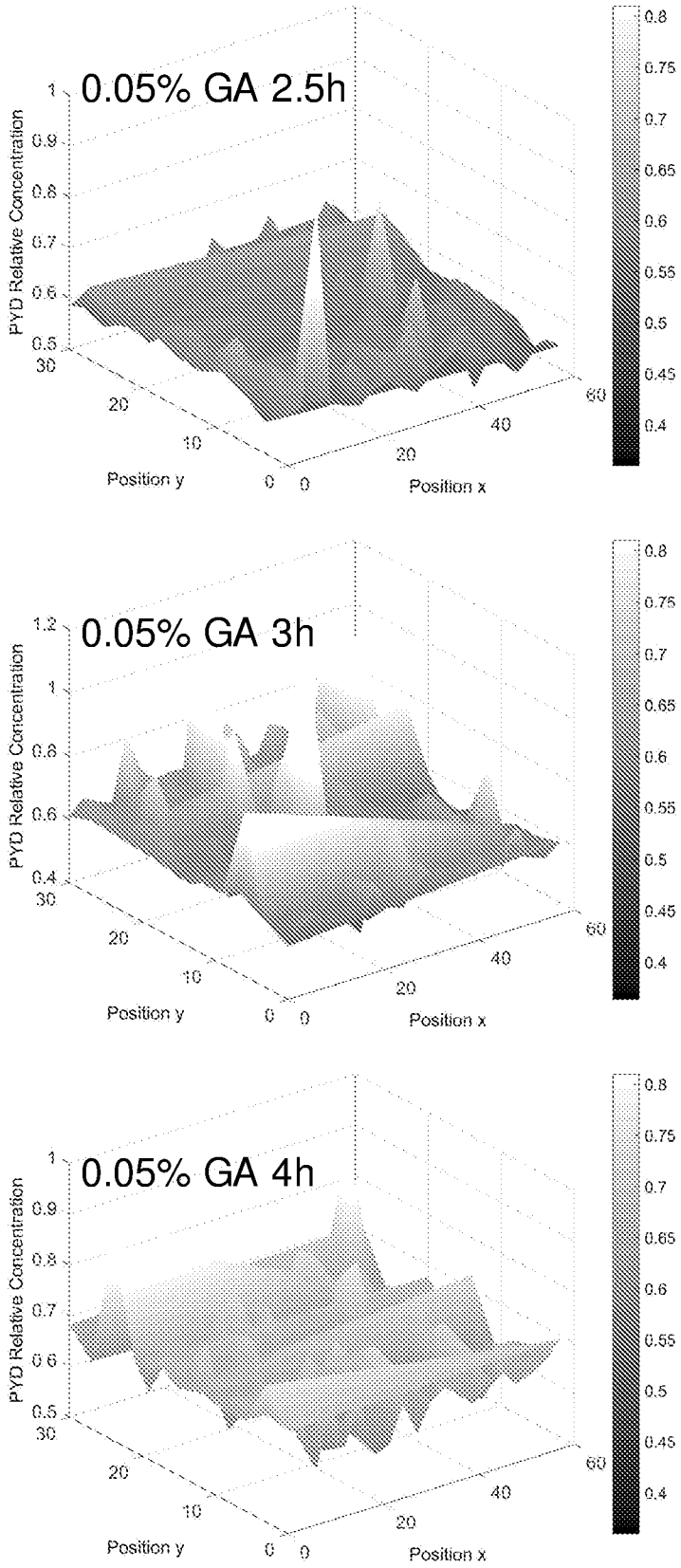

0.05% GA 2.5h
PYD Relative Concentration
1
0.9
0.8
0.7
0.6
0.5
30
20
10
0
Position y
0
20
40
60
Position x
0.8
0.75
0.7
0.65
0.6
0.55
0.5
0.45
0.4
0.05% GA 3h
PYD Relative Concentration
1.2
1
0.8
0.6
0.4
30
20
10
0
Position y
0
20
40
60
Position x
0.8
0.75
0.7
0.65
0.6
0.55
0.5
0.45
0.4
0.05% GA 4h
PYD Relative Concentration
1
0.9
0.8
0.7
0.6
0.5
30
20
10
0
Position y
0
20
40
60
Position x
0.8
0.75
0.7
0.65
0.6
0.55
0.5
0.45
0.4

Fig. 6C

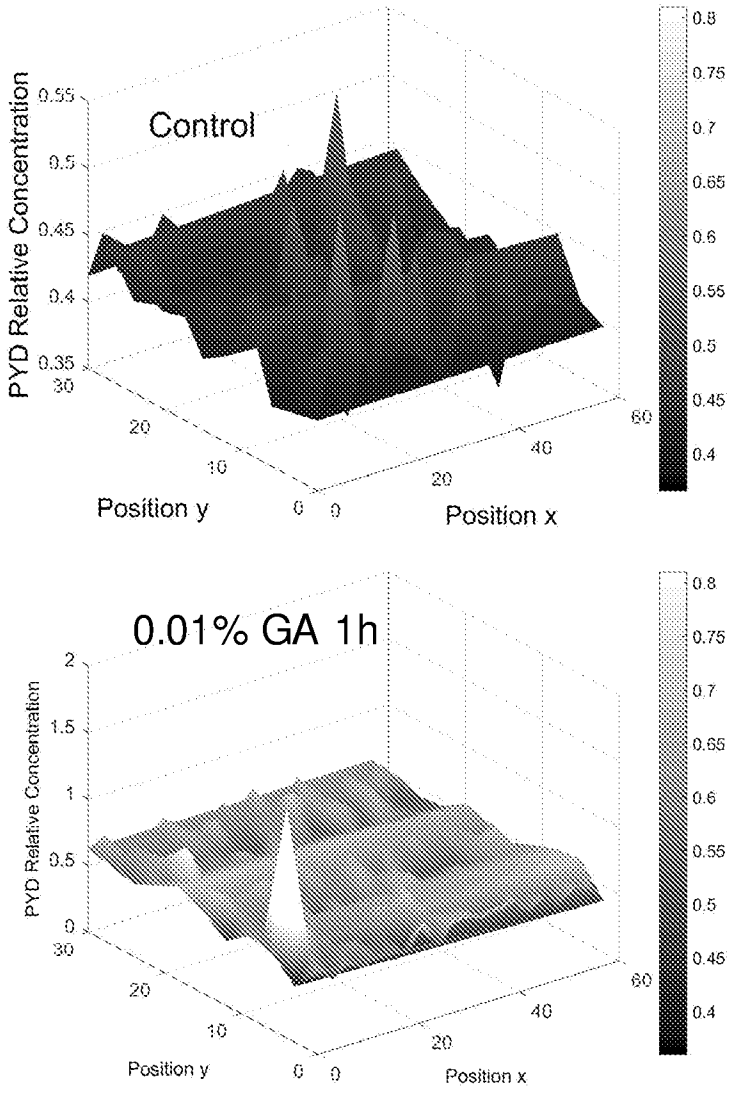

Control
PYD Relative Concentration
0.55
0.5
0.45
0.4
0.35
30
20
10
0
Position y
0
20
40
60
Position x
0.8
0.75
0.7
0.65
0.6
0.55
0.5
0.45
0.4
0.01% GA 1h
PYD Relative Concentration
2
1.5
1
0.5
0
30
20
10
0
Position y
0
20
40
60
Position x
0.8
0.75
0.7
0.65
0.6
0.55
0.5
0.45
0.4

Fig. 6D

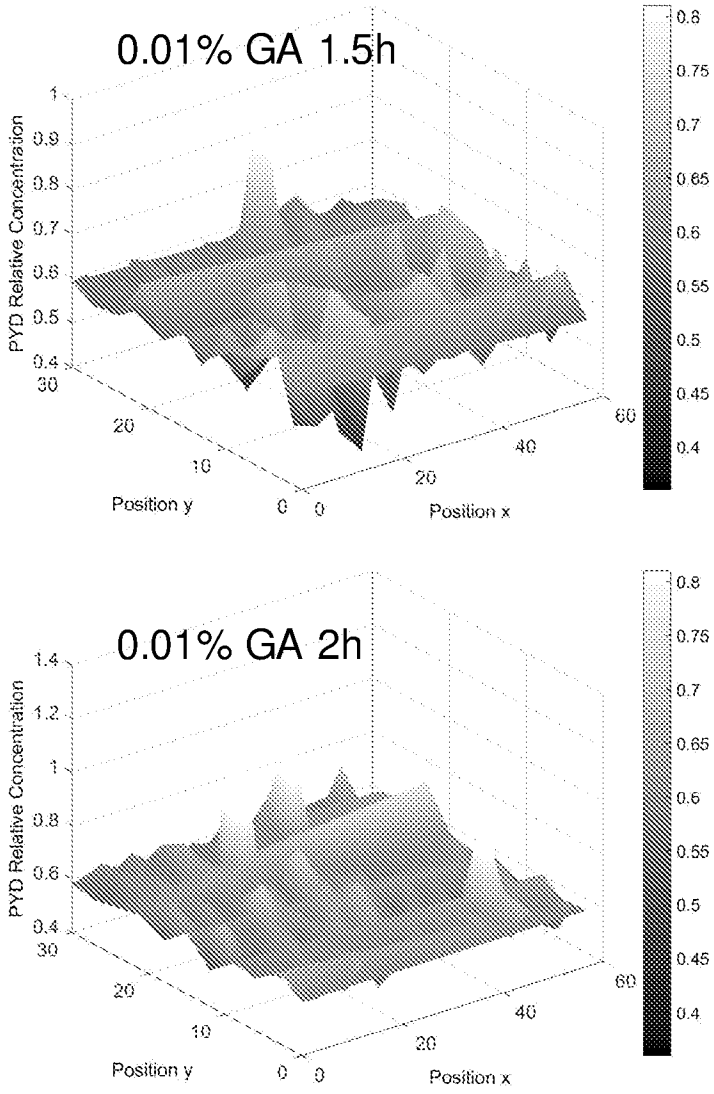

0.01% GA 1.5h
PYD Relative Concentration
1
0.9
0.8
0.7
0.6
0.5
0.4
30
20
10
0
Position y
0
20
40
60
Position x
0.8
0.75
0.7
0.65
0.6
0.55
0.5
0.45
0.4
0.01% GA 2h
PYD Relative Concentration
1.4
1.2
1
0.8
0.6
0.4
30
20
10
0
Position y
0
20
40
60
Position x
0.8
0.75
0.7
0.65
0.6
0.55
0.5
0.45
0.4

Fig. 6E

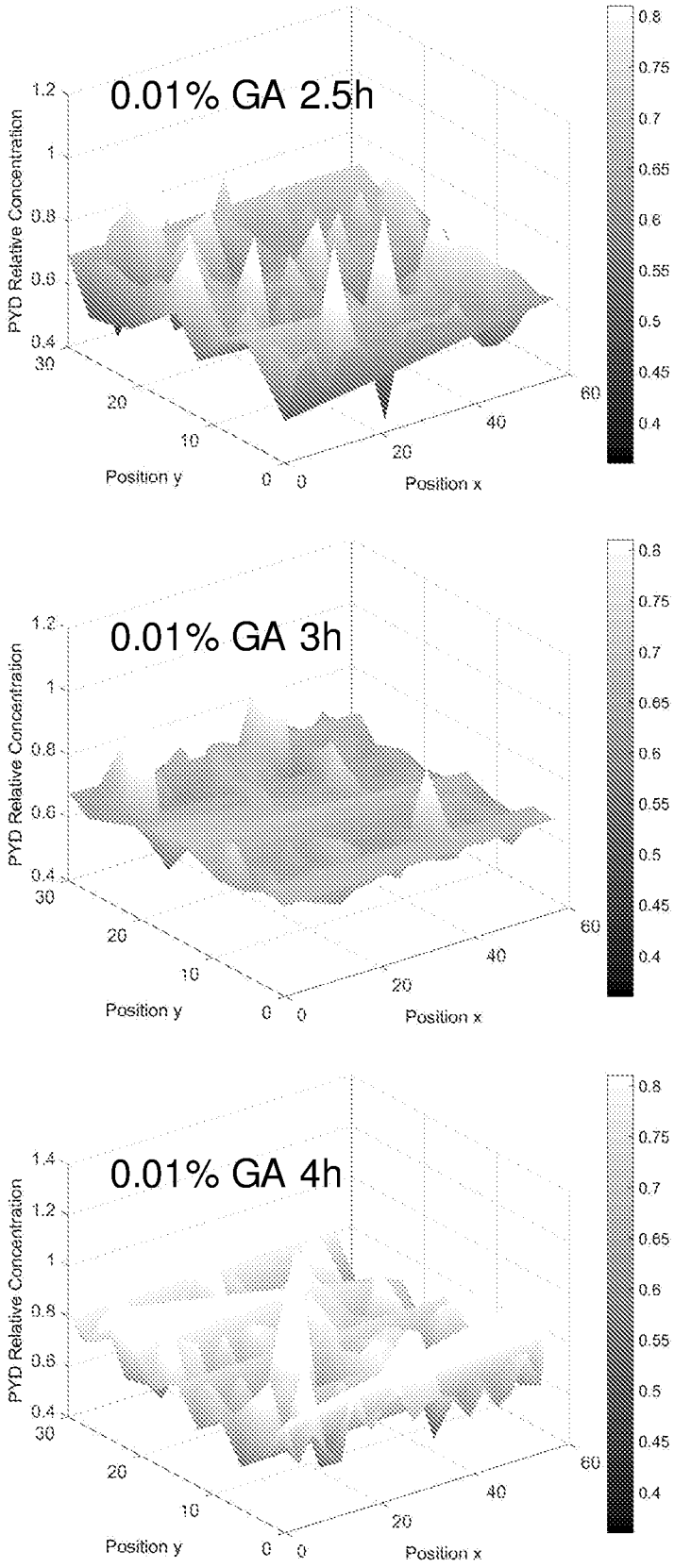

0.01% GA 2.5h
PYD Relative Concentration
1.2
1
0.8
0.6
0.4
30
20
10
0
Position y
0
20
40
60
Position x
0.8
0.75
0.7
0.65
0.6
0.55
0.5
0.45
0.4
0.01% GA 3h
PYD Relative Concentration
1.2
1
0.8
0.6
0.4
30
20
10
0
Position y
0
20
40
60
Position x
0.8
0.75
0.7
0.65
0.6
0.55
0.5
0.45
0.4
0.01% GA 4h
PYD Relative Concentration
1.4
1.2
1
0.8
0.6
0.4
30
20
10
0
Position y
0
20
40
60
Position x
0.8
0.75
0.7
0.65
0.6
0.55
0.5
0.45
0.4

Fig. 6F

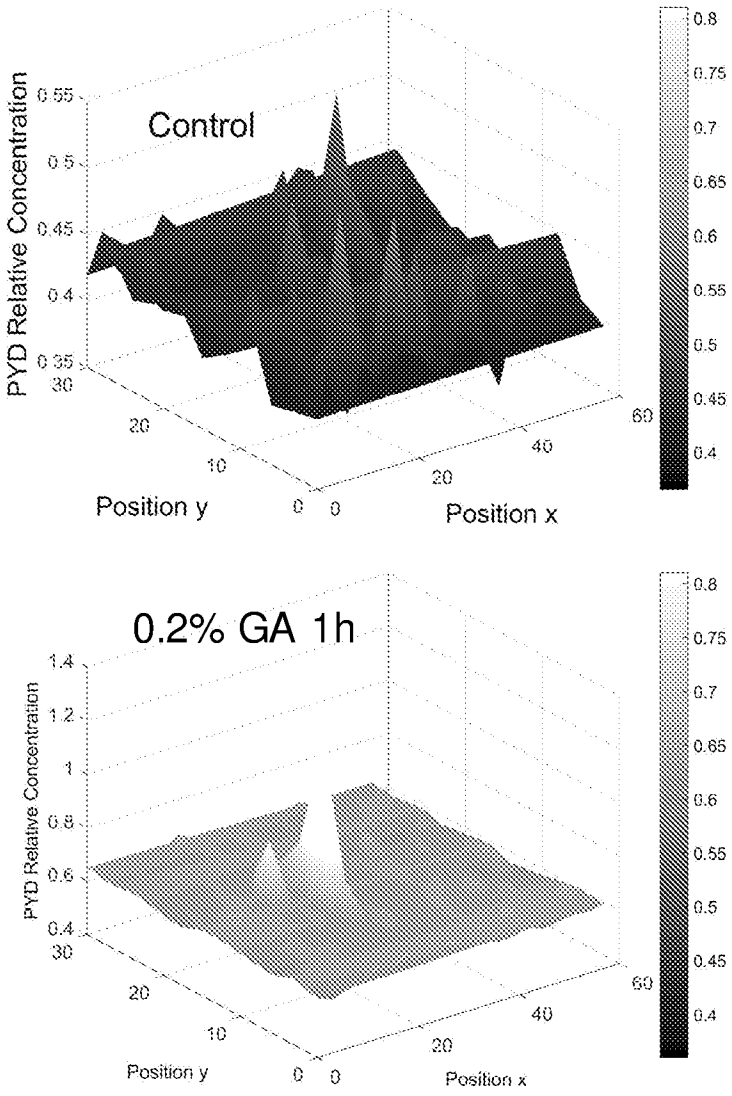

Control
PYD Relative Concentration
0.55
0.5
0.45
0.4
0.35
30
20
10
0
Position y
0
20
40
60
Position x
0.8
0.75
0.7
0.65
0.6
0.55
0.5
0.45
0.4
0.2% GA 1h
PYD Relative Concentration
1.4
1.2
1
0.8
0.6
0.4
30
20
10
0
Position y
0
20
40
60
Position x
0.8
0.75
0.7
0.65
0.6
0.55
0.5
0.45
0.4

Fig. 6G

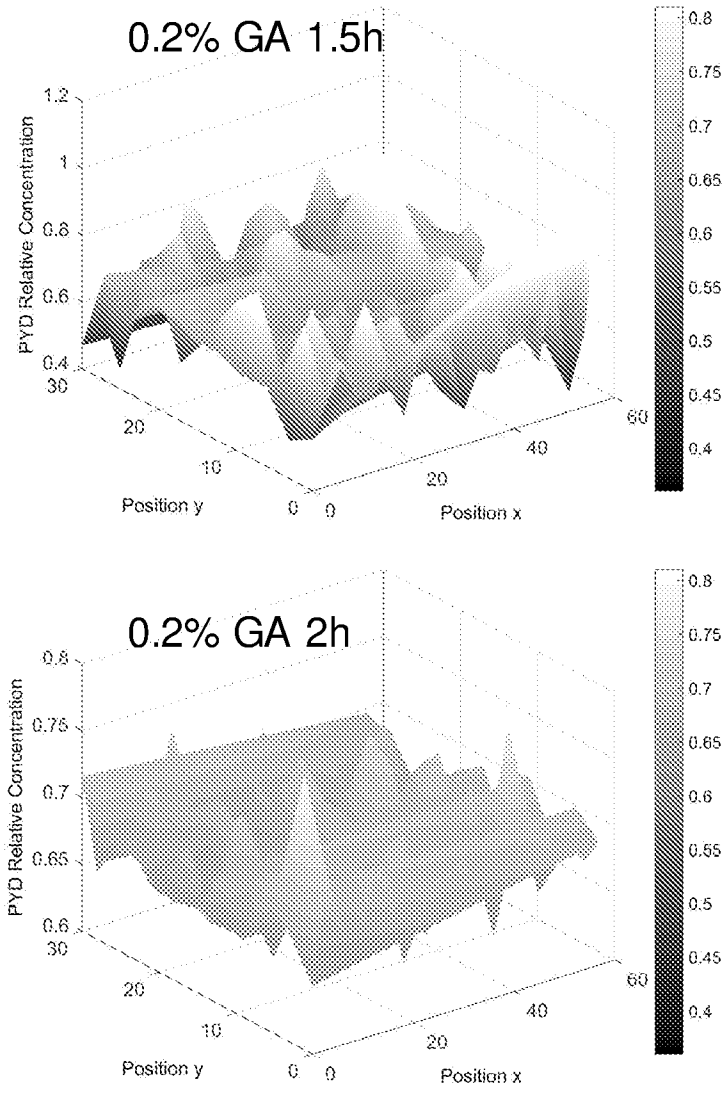

0.2% GA 1.5h
PYD Relative Concentration
1.2
1
0.8
0.6
0.4
30
20
10
0
Position y
0
20
40
60
Position x
0.8
0.75
0.7
0.65
0.6
0.55
0.5
0.45
0.4
0.2% GA 2h
PYD Relative Concentration
0.8
0.75
0.7
0.65
0.6
30
20
10
0
Position y
0
20
40
60
Position x
0.8
0.75
0.7
0.65
0.6
0.55
0.5
0.45
0.4

Fig. 6H

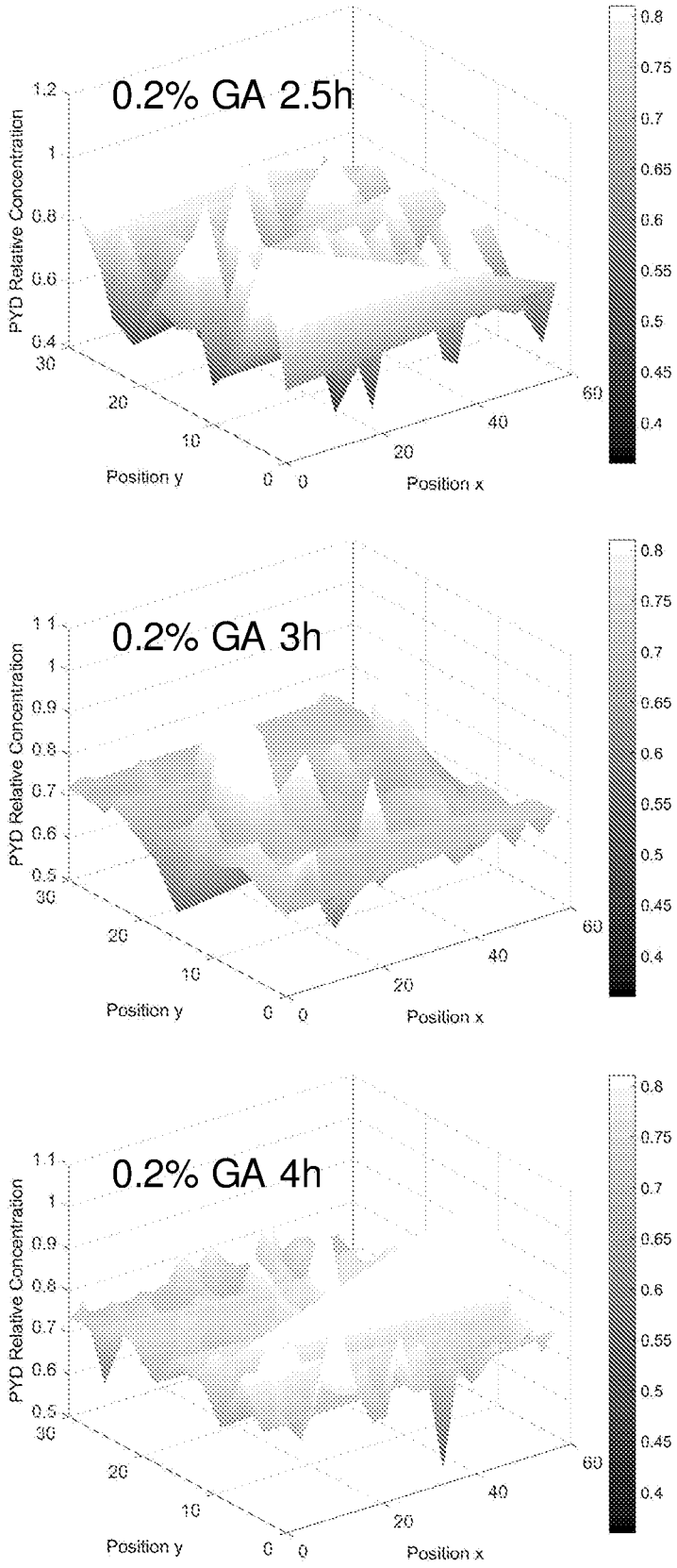

0.2% GA 2.5h
PYD Relative Concentration
1.2
1
0.8
0.6
0.4
30
20
10
0
Position y
0
20
40
60
Position x
0.8
0.75
0.7
0.65
0.6
0.55
0.5
0.45
0.4
0.2% GA 3h
PYD Relative Concentration
1.1
1
0.9
0.8
0.7
0.6
0.5
30
20
10
0
Position y
0
20
40
60
Position x
0.8
0.75
0.7
0.65
0.6
0.55
0.5
0.45
0.4
0.2% GA 4h
PYD Relative Concentration
1.1
1
0.9
0.8
0.7
0.6
0.5
30
20
10
0
Position y
0
20
40
60
Position x
0.8
0.75
0.7
0.65
0.6
0.55
0.5
0.45
0.4

Fig. 6J

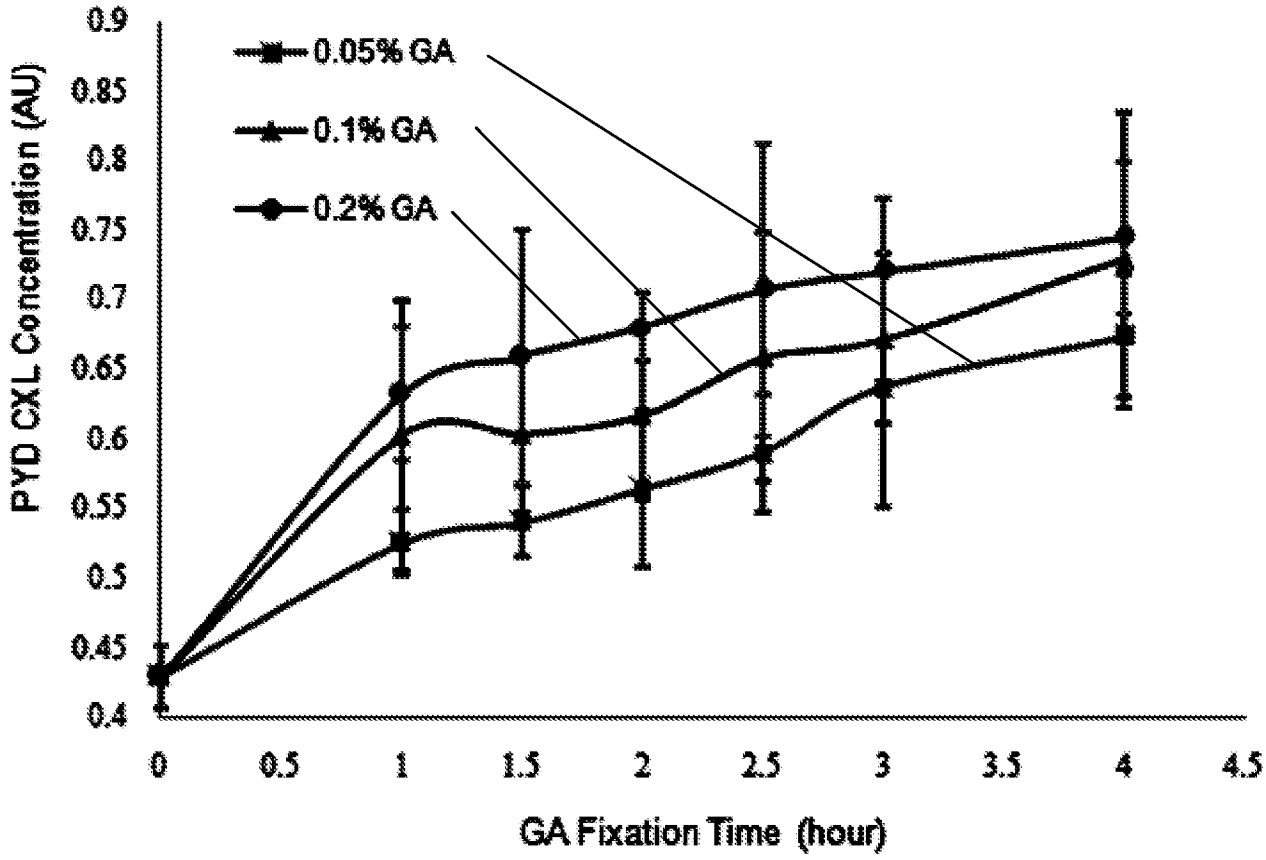

0.05% GA
0.1% GA
0.2% GA
PYD CXL Concentration (AU)
0.9
0.85
0.8
0.75
0.7
0.65
0.6
0.55
0.5
0.45
0.4
0
0.5
1
1.5
2
2.5
3
3.5
4
4.5
GA Fixation Time (hour)

Fig. 7

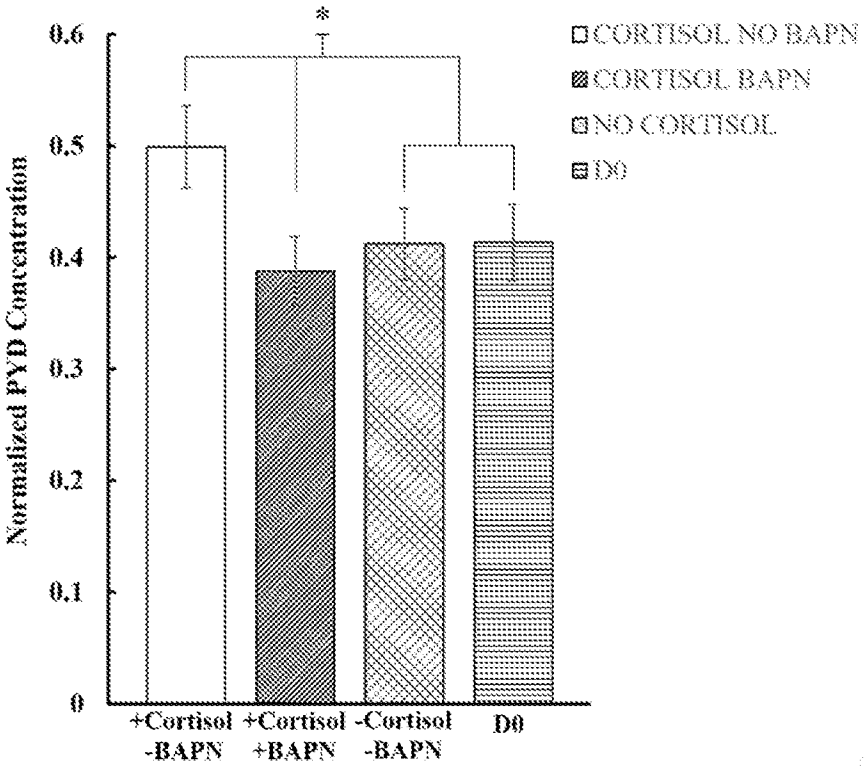

*
CORTISOL NO BAPN
CORTISOL BAPN
NO CORTISOL
D0
Normalized PYD Concentration
0.6
0.5
0.4
0.3
0.2
0.1
0
+Cortisol -BAPN
+Cortisol +BAPN
-Cortisol -BAPN
D0

Fig. 8A

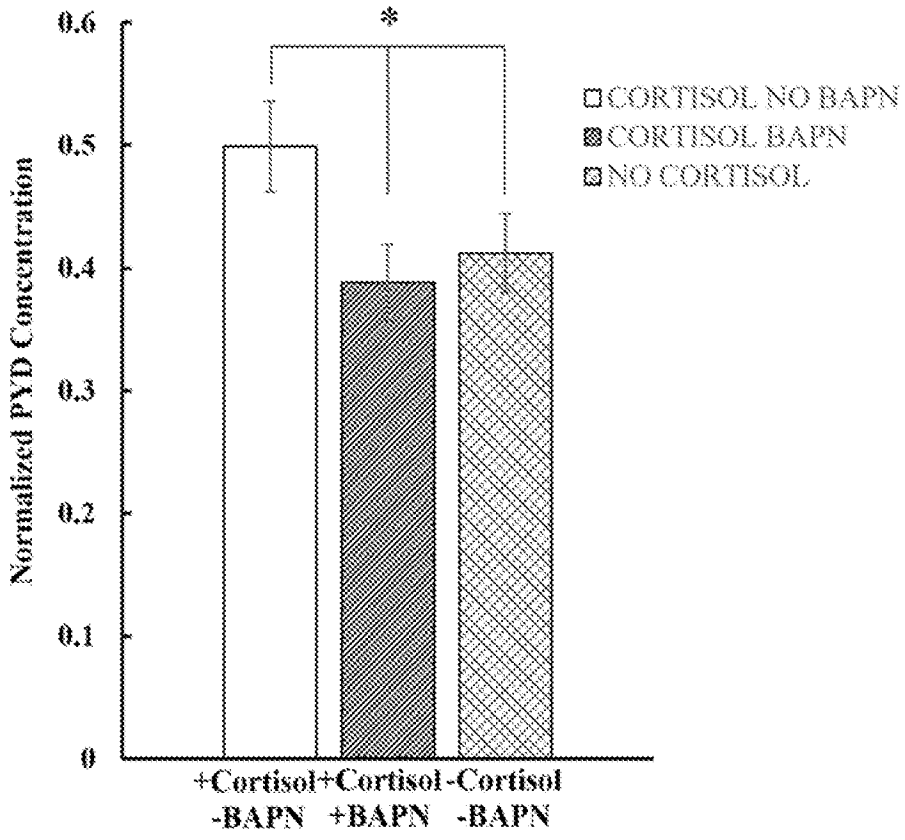

*
CORTISOL NO BAPN
CORTISOL BAPN
NO CORTISOL
Normalized PYD Concentration
0.6
0.5
0.4
0.3
0.2
0.1
0
+Cortisol -BAPN
+Cortisol +BAPN
-Cortisol -BAPN

Fig. 8B

INTERNATIONAL SEARCH REPORT

International application No.
PCT/US2017/036915

A. CLASSIFICATION OF SUBJECT MATTER
IPC(8) - A61B 5/00; G01J 3/00; G01J 3/44 (2017.01)
CPC - A61B 5/4514; A61B 5/00; A61B 5/45; G01J 3/00; G01J 3/44 (2017.08)

According to International Patent Classification (IPC) or to both national classification and IPC

B. FIELDS SEARCHED

Minimum documentation searched (classification system followed by classification symbols)
See Search History document

Documentation searched other than minimum documentation to the extent that such documents are included in the fields searched

Electronic data base consulted during the international search (name of data base and, where practicable, search terms used)
See Search History document

C. DOCUMENTS CONSIDERED TO BE RELEVANT

Category*	Citation of document, with indication, where appropriate, of the relevant passages	Relevant to claim No.
X --- Y	WANG et al., Quantitative Raman Characterization of Cross-linked Collagen Thin Films as a Model System for Diagnosing Early Osteoarthritis, Proceedings Volume 9704, Biomedical Vibrational Spectroscopy 2016: Advances in Research and Industry, 970415, 07 March 2016 [retrieved on 04 October 2017]. Retrieved from the Internet: <URL: https://www.spiedigitallibrary.org/conference-proceedings-of-spie/9704/1/Quantitative-Raman-characterization-of-cross-linked-collagen-thin-films-as/10.1117/12.2228328.pdf?SSO=1>. entire document	1-5, 11-18, 21, 22 --- 6-10, 19, 20
Y	ESMONDE-WHITE et al., Fiber-optic Raman Spectroscopy of Joint Tissues, Analyst. Vol. 136, No. 8, 21 April 2012 [retrieved on 04 October 2017]. Retrieved from the Internet: <URL: https://www.ncbi.nlm.nih.gov/pmc/articles/PMC3108821/>. entire document	6-10, 19, 20
A	US 2007/0049808 A1 (ROESSLER et al) 01 March 2007 (01.03.2007) entire document	1-22

☐ Further documents are listed in the continuation of Box C. ☐ See patent family annex.

* Special categories of cited documents:
"A" document defining the general state of the art which is not considered to be of particular relevance
"E" earlier application or patent but published on or after the international filing date
"L" document which may throw doubts on priority claim(s) or which is cited to establish the publication date of another citation or other special reason (as specified)
"O" document referring to an oral disclosure, use, exhibition or other means
"P" document published prior to the international filing date but later than the priority date claimed
"T" later document published after the international filing date or priority date and not in conflict with the application but cited to understand the principle or theory underlying the invention
"X" document of particular relevance; the claimed invention cannot be considered novel or cannot be considered to involve an inventive step when the document is taken alone
"Y" document of particular relevance; the claimed invention cannot be considered to involve an inventive step when the document is combined with one or more other such documents, such combination being obvious to a person skilled in the art
"&" document member of the same patent family

Date of the actual completion of the international search	Date of mailing of the international search report
04 October 2017	23 OCT 2017
Name and mailing address of the ISA/US Mail Stop PCT, Attn: ISA/US, Commissioner for Patents P.O. Box 1450, Alexandria, VA 22313-1450 Facsimile No. 571-273-8300	Authorized officer Blaine R. Copenheaver PCT Helpdesk: 571-272-4300 PCT OSP: 571-272-7774

Form PCT/ISA/210 (second sheet) (January 2015)

INTERNATIONAL SEARCH REPORT

International application No.
PCT/US2017/036915

Box No. II Observations where certain claims were found unsearchable (Continuation of item 2 of first sheet)

This international search report has not been established in respect of certain claims under Article 17(2)(a) for the following reasons:

1. ☐ Claims Nos.:
because they relate to subject matter not required to be searched by this Authority, namely:

2. ☐ Claims Nos.:
because they relate to parts of the international application that do not comply with the prescribed requirements to such an extent that no meaningful international search can be carried out, specifically:

3. ☐ Claims Nos.:
because they are dependent claims and are not drafted in accordance with the second and third sentences of Rule 6.4(a).

Box No. III Observations where unity of invention is lacking (Continuation of item 3 of first sheet)

This International Searching Authority found multiple inventions in this international application, as follows:

See Extra Sheet

1. ☐ As all required additional search fees were timely paid by the applicant, this international search report covers all searchable claims.

2. ☐ As all searchable claims could be searched without effort justifying additional fees, this Authority did not invite payment of additional fees.

3. ☐ As only some of the required additional search fees were timely paid by the applicant, this international search report covers only those claims for which fees were paid, specifically claims Nos.:

4. ☐ No required additional search fees were timely paid by the applicant. Consequently, this international search report is restricted to the invention first mentioned in the claims; it is covered by claims Nos.:

Remark on Protest

☐ The additional search fees were accompanied by the applicant's protest and, where applicable, the payment of a protest fee.

☐ The additional search fees were accompanied by the applicant's protest but the applicable protest fee was not paid within the time limit specified in the invitation.

☐ No protest accompanied the payment of additional search fees.

INTERNATIONAL SEARCH REPORT

International application No.
PCT/US2017/036915

Continued from Box No. III Observations where unity of invention is lacking

This application contains the following inventions or groups of inventions which are not so linked as to form a single general inventive concept under PCT Rule 13.1. In order for all inventions to be examined, the appropriate additional examination fees must be paid.

Group I, claims 1-22, drawn to a method of analyzing Raman spectral data from collagen.
Group II, claims 1-12,23-25, drawn to a method of diagnosing osteoarthritis.
Group III, claims 1-12,26-29, drawn to a system for diagnosing osteoarthritis.

The inventions listed as Groups I, II and III do not relate to a single general inventive concept under PCT Rule 13.1 because, under PCT Rule 13.2, they lack the same or corresponding special technical features for the following reasons: the special technical feature of the Group I invention: extracting information from the model indicative of changes in relative concentration of CxLs; and quantitatively assessing changes in relative concentration of CxLs induced by glutaraldehyde fixation to diagnose the osteoarthritis as claimed therein is not present in the invention of Groups II and III. The special technical feature of the Group II invention: generating a display of spatially-resolved magnitudes of cross-linking responsively to said quantifying as claimed therein is not present in the invention of Groups I or III. The special technical feature of the Group III invention: a machine classifier programmed to distinguish between healthy and arthritic cartilage from said reduced spectral data and to output an indication responsive to a detected class as claimed therein is not present in the invention of Groups I or II.

Groups I, II and III lack unity of invention because even though the inventions of these groups require the technical feature of generating a Raman spectrum of cartilage tissue; and measuring one or more Raman spectrum peaks, this technical feature is not a special technical feature as it does not make a contribution over the prior art.

Specifically, US 2007/0049808 A1 (ROESSLER et al) 01 March 2007 (01.03.2007) teaches generating a Raman spectrum of cartilage tissue (Paras. 10-12); and measuring one or more Raman spectrum peaks (Paras. 159-160).

Since none of the special technical features of the Group I, II or III inventions are found in more than one of the inventions, unity of invention is lacking.